

Extension of the eSAFT-VR Mie equation of state from aqueous to non-aqueous electrolyte solutions

Nefeli Novak^{a,b}, Georgios M. Kontogeorgis^b, Marcelo Castier^{c,#}, Ioannis G. Economou^{a,c,*}

^a National Center for Scientific Research "Demokritos", Institute of Nanoscience and Nanotechnology, Molecular Thermodynamics and Modeling of Materials Laboratory, GR – 153 10, Aghia Paraskevi, Attikis, Greece

^b Center for Energy Resources Engineering, Department of Chemical and Biochemical Engineering, Technical University of Denmark, 2800, Kgs Lyngby, Denmark

^c Texas A&M University at Qatar, Chemical Engineering Program, Education City, PO Box 23874, Doha, Qatar

ABSTRACT

In this work, the eSAFT-VR Mie equation of state (EoS) is extended to low relative permittivity, non-aqueous solutions. The effect of using different relative permittivity relations for the electrolyte solutions is studied, ranging from experimentally measured values to a salt-composition independent relative permittivity. Furthermore, the effect of using different approaches for the characteristic diameters in the Debye-Hückel and Born terms is presented. The eSAFT-VR Mie EoS is reparametrized using aqueous mean ionic activity coefficients, individual ion activity coefficients and densities with different relations for the relative permittivity. Afterwards, the performance of these models on non-aqueous solutions is evaluated based on the Mean Ionic Activity Coefficients of salts in non-aqueous solutions. The conclusion is that a mole fraction based mixing rule for the relative permittivity yields the best extrapolation from aqueous to non-aqueous solutions, and achieves quantitative predictions for the mean ionic activity coefficients of monovalent salts in methanol and ethanol without additional adjustable parameters.

1. Introduction

Electrolyte thermodynamics is constantly gaining interest due to an increasingly wide range of applications of electrolyte solutions. Typical examples of aqueous electrolyte solution processes are water purification and scaling. Furthermore in this category belong all processes that involve immiscible systems where the electrolyte is present in the aqueous phase only, such as carbon capture utilization and/or sequestration (CCUS) [1,2], and oil and gas production from conventional [3] and unconventional [4,5] reservoirs. The participation of mixed-solvent systems or even non-aqueous electrolyte solutions in innovative applications, such as power generation through reverse electrodialysis [6], fuel cell technology [7] and lithium batteries [8], enhances the need for accurate thermodynamic description of such mixtures as well.

There are many electrolyte Equations of State (eEoS) that have proven to be successful for modeling aqueous solutions, which vary significantly in their formulation because of unresolved fundamental issues related to electrolyte thermodynamics. Walker et al. [9] presented an investigation of various aspects of electrolyte modeling including the effect of parameterization, relative permittivity model, electrostatic interaction model (Debye-Hückel, DH in brief, and Mean Spherical Approximation, MSA in brief) for aqueous solutions, within the context

of eSAFT-VR Mie. An important conclusion of this work [9] is the high sensitivity of the models to the relative permittivity relation, which is quickly becoming one of the most influential and controversial topics in electrolyte EoS modeling [9–11].

Two reasons can be identified for the controversy regarding the relative permittivity: a fundamental one concerning the derivation of the ion-ion terms and a more practical one concerning the experimental relative permittivity of electrolyte solutions. It has been debated that since the ion-ion interactions are derived using the McMillan-Mayer framework, the solvent should be treated as a continuum with constant macroscopic properties (such as density and relative permittivity) [12–14]. However, in the book by Michelsen and Møllerup, this constraint is afterwards relaxed, and it is suggested that a salt-composition-dependent relative permittivity can be used within the context of EoS [14]. Also, according to Ahmed et al. [15], since the Born term accounts for charging an ion in a dielectric medium, the relative permittivity that is used within this term has to be salt-composition-dependent. To add to this ambiguity, experimental measurements of relative permittivity are actually a result of two distinct contributions [16]: kinetic depolarization (movement of ions due to the external electric field enforced during the measurements) and dielectric saturation (water molecules in the solvation shells are unable

* Corresponding author.

E-mail address: ioannis.economou@qatar.tamu.edu (I.G. Economou).

Work done, in part, while at Universidad Paraguayo Alemana, San Lorenzo, Paraguay.

Table 1

Summary of electrolyte EoS from the literature.

Model	Relative Permittivity	Adjustable Parameters	Fitted Properties
eSAFT-VRE			
Schreckenberget al. ¹	Schreckenberget al. ¹	$\sigma_{ion}, \epsilon_{ion}, IP_{ion,water}(\epsilon_{ion,water})$	VLE, ρ, γ^{\pm}
eSAFT-VR Mie			
Selam et al. ²	Constant	$\sigma_{ion}, IP_{ion,water}(\epsilon_{ion,water})$	ρ, γ^{\pm}
Eriksen et al. ³	Schreckenberget al. ¹	$IP_{ion,water}(\epsilon_{ion,water})$	VLE, ρ, Φ
ePC-SAFT			
Held et al. ⁴	Constant	σ_{ion}, u_{ion}	ρ, γ^{\pm}
Held et al. ^{5*}	Constant	$\sigma_{ion}, u_{ion}, IP(k_{ion,water}, k_{ion,ion}, k_{ion,solvent}, l_{ion,solvent})$	ρ, Φ
Held et al. ^{6**}	Constant	$\sigma_{ion}, u_{ion}, \text{solvent specific } \sigma_{ion}, u_{ion}, IP(k_{ion,ion})$	ρ, γ^{\pm}, Φ
Bülow et al. ^{7**}	Mole fraction mixing rule ⁷	Parameters taken from previous implementation of the model ⁵ for aqueous solution, while $k_{ion,ion}$ is assumed zero.	—
ePPC-SAFT			
Rozmus et al. ⁸	Pottel model	ϵ_{ion}^{AB}	v^{app}, γ^{\pm}
Ahmed et al. ^{9*}	Pottel model	$\sigma_{MSA, ion}, \epsilon_{ion}^{AB}$	ρ, γ^{\pm}
Pinto et al. ⁹	Schreckenberget al., Simonin	Various adjustable parameters	$\gamma^{\pm}, \Phi, v^{app}, \Delta h^{sol}$
eCPA			
Maribo-Mogensen et al. ^{10*}	Maribo-Mogensen et al. ¹¹	$IP_{ion,water}(\Delta U_{salt,water}, \alpha_{salt}, T_{a,salt}), c_{ion}, R_{Born, ion}$	$\gamma^{\pm}, \Phi, \Delta h^{hyd}$ for Born diameter ($R_{Born, ion}$), ρ for Peneloux parameter (c_{ion})
Schlaikjer et al. ^{12*}	Maribo-Mogensen et al. ¹¹	$IP_{ion,water}(\Delta U_{salt,water}, \alpha_{salt}, T_{a,salt}), \Gamma_{ion}, \sigma_{ion}, c_{ion} [c_{ion}, R_{Born, ion}^{10}]$	$\gamma^{\pm}, \Phi, SLE, \rho$
Olsen et al. ¹³	Maribo-Mogensen et al. ¹¹	$IP_{ion,water}(\Delta U_{salt,water}, \alpha_{salt}, T_{a,salt}), \sigma_{ion} [R_{Born, ion} \text{ from }^{10}]$	γ^{\pm}, Φ, ρ
Other models			
Zuber et al. ^{14**}	Zuber et al. ¹⁵	$\sigma_{ion}, \text{solvent specific}, IP_{ion,solvent}(u_{ion,solvent})$	VLE, γ^{\pm}, ρ
Zuo and Fürst ^{16**}	Zuo and Fürst ¹⁶	Various approaches	VLE, γ^{\pm}

Abbreviations: γ^{\pm} : MIAC, Φ : osmotic coefficient, ρ : density, v^{app} : apparent molar volume, Δh^{sol} : solution enthalpy, Δh^{hyd} : hydration enthalpy, VLE: Vapor pressure, SLE: salt solubility, IP: interaction parameter, different type depending on the model

* : application in mixed solvents.

** : application in non-aqueous solvents.

Table 2Correlations for the relative permittivity of pure solvents (ϵ_r^{pure}) with temperature (T in K) [38].

Solvent	ϵ_r^{pure}
Water	$-19.2905 + \frac{29814.5}{T} - 0.019678 T + \frac{0.013189}{10^2} T^2 - \frac{0.031144}{10^5} T^3$
Methanol	$10^{1.514 - 0.00264(T - 298.15)}$
Ethanol	$175.72 - \frac{3.0699}{T} - 0.35350 T - \frac{0.20285}{10^2} T^2 + \frac{0.50644}{10^5} T^3$

to rotate according to an external electric field and are effectively not contributing to the relative permittivity of the solution). Kinetic depolarization contributes to the 25-75% of the decrease in the permittivity [16].

The confusion regarding relative permittivity stems from the fact that it is not resolved whether a salt-composition-dependent or independent- relative permittivity value should be used within EoS frameworks and, on top of that, the thermodynamic contribution (dielectric relaxation) cannot be measured due to the kinetic depolarization. On the

other hand, the static permittivity is a required input in the DH [17] theory and the Born [18] theory for primitive models. Apart from the correct value of the relative permittivity, its derivatives are also important as they influence the DH and Born contributions in the mean ionic activity coefficient [9,15,19,20], second derivative properties [9], as well as chemical and phase equilibrium in mixed-solvent electrolyte solutions [21]. Using empirical models for the relative permittivity within the framework of thermodynamic models may introduce unphysical behavior [22].

Within the EoS community, there are different approaches with respect to the relative permittivity. In the non-primitive approach, the static relative permittivity of the solution is calculated by the EoS, and it is therefore an output of thermodynamic modeling [23–26]. One such work focusing on non-aqueous and mixed solvent solutions is that of Das et al. [25]. On the other hand, in the primitive approach, the relative permittivity is an input for the EoS. Within this framework, some models utilize a constant value of the relative static permittivity equal to that of the solvent [27–29]. Another approach adopted by many models is the Schreckenberget al. [30,31], where the relative permittivity used in EoS is in principle that of the solvent, but it is calculated as a function of

Table 3

Pure component parameters of SAFT-VR Mie used in this work.

Component	m	$\sigma(\text{\AA})$	λ_r^a	$\epsilon/k_B(K)$	$\epsilon_{ab}^{HB}/k_B(K)$	$K_{ab}(\text{\AA}^3)$	Association scheme
Water[48]	1	3.0555	35.823	418	1600	496.66	4C
Methanol[48]	1.7989	3.1425	16.968	276.92	2156	222.18	3B
Ethanol ^b	1.6539	3.685	15.4738	299.2	2672.4	156.51	2B

^a : $\lambda_a = 6$ in all solvents.

^b : Determined in this study by fitting vapor pressure (AARD=0.5%) and liquid density (AARD=0.2%) in the range 230-488 K. AARD% =

$$\frac{100}{NP} \sum_{i=1}^{NP} \left(\frac{|prop^{exp} - prop^{calc}|}{prop^{exp}} \right).$$

Table 4

Mean Ionic Activity Coefficient data sources for single salts in non-aqueous solvents reported in the literature.

Potentiometric methods		
NaF	methanol, ethanol	Hernández-Luis et al., 2003 [72]
NaCl	methanol	Yan et al., 1995 [73]
NaCl	90% ethanol, 10% water	Esteso et al., 1989 [74]
NaBr	methanol, ethanol	Han & Pan, 1993 [75]
NaBr	ethanol	Gonzalez-Diaz et al., 1995 [76]
KCl	methanol	Malahias & Popovych, 1982 [77]
Vapor pressure methods		
NaCl, NaBr	methanol	Vlasov & Antonov, 1973 [78]
NaI	ethanol, 2-propanol, acetonitrile	Barthel & Lauermaun, 1986 [56]
KBr	methanol	Kolhapurkar et al., 2006 [79]
LiCl, LiBr, LiI, NaBr, NaI	methanol, ethanol	Held et al., 2012 [42]
LiCl, LiBr	methanol	Skabichevskii, 1969 [71]
LiCl, LiBr	methanol	Safarov, 2005 [69]
LiCl, LiBr	ethanol	Safarov, 2006 [67]
LiCl, LiBr	DMSO, acetonitrile	Xin et al., 2019 [8]
LiCl, LiBr	2-propanol	Zafarani-Moattar & Aria, 2001 [70]
LiBr	acetone	Barthel et al., 1999 [60]
LiBr	methanol	Nasirzadeh et al., 2004 [63]
LiBr	ethanol	Nasirzadeh et al., 2004 [64]
LiBr	2-propanol	Nasirzadeh et al., 2005 [65]
Solubility methods		
KCl, KBr, NaCl	DMSO	Long et al., 2011 [80]
KI	acetone, ethanol, 1-propanol	Long et al., 2012 [55]
LiBr	methanol, ethanol, 1-propanol, 2-propanol and 1-butanol	Li et al., 2011 [81]

the density and temperature. In this case, there is a mild dependence of the mixture relative permittivity on the salt concentration, as shown by Walker et al. [9]. Similar solution relative permittivity is achieved using a simple mole fraction mixing rule proposed by Bülow et al. [10]. Various correlations of experimental data have also been used, such as the relations by Breil, Michelsen and Møllerup [14], Zuber et al. [32], or the Simonin model [33]. Models with a theoretical basis, such as the Pottel model [15,34] and the Maribo-Mogensen model [20,35] have also been implemented in electrolyte EoS (eEoS). Most of these relative permittivity relations have been used in the framework of eEoS in the literature, although their application has been mostly limited to single solvent, aqueous solutions. A recent direct comparison of various relative permittivity relations in the context of ePPC-SAFT shows that the effect of using different relative permittivity relations in the eEoS predictions of various properties of aqueous electrolyte solutions is

absorbed by the model's adjustable parameters [36].

Up to recently, the discussion in the literature has been limited to aqueous solutions. The different focus in insight and modeling work between water and other solvents has been recently illustrated by Held [37] in a review paper on modeling electrolyte solutions in water-poor media. In this review paper, Held pinpointed that although several electrolyte models exist in the literature, they are either still restricted to aqueous solutions or their extension to non-aqueous solutions requires complete reparameterization and sometimes even solvent-dependent parameters. According to the author [37], the reason for the inability of models to be extended to non-aqueous solutions is due to invalid expressions for the permittivity, the constraint to use salt-specific model parameters, the assumption of complete dissociation of an electrolyte into its ions, and neglecting Born term or Gibbs energies of transfer when an additional liquid phase is present.

Zuo and Fürst [38] were the first ones to present predictive results in non-aqueous solvents. They extended the Fürst and Renon EoS to predict vapor pressures and mean activity coefficients of binary non-aqueous electrolyte systems by use of the two methods; in method I, they kept the same parameters as determined for aqueous solutions, while using the Stokes cationic diameters that are different for each solvent, but

Table 5

Database of MIAC of salts in aqueous and non-aqueous electrolyte solutions at 298.15 K and atmospheric pressure used in this work.

Solvent	Salt	Number of Data Points	Reference
Water	LiCl	19	[83]
	LiBr	10	[83]
	LiI	23	[83]
	NaCl	53	[83]
	NaBr	47	[83]
	NaI	4	[83]
	KCl	38	[83]
	KBr	32	[83]
	KI	7	[83]
	LiCl	62	[69,71,84,85]
Methanol	LiBr	48	[69,71,84]
	LiI	5	[42]
	NaCl	25	[73,85]
	NaBr	27	[75,78]
	NaI	13	[56]
	KCl	11	[77]
	KBr	7	[79]
	KI	10	[85]
	LiCl	25	[42,67,85]
	LiBr	35	[64,67,86]
Ethanol	LiI	5	[42]
	NaCl	10	[42,74]
	NaBr	31	[42,75,76]
	NaI	20	[56]

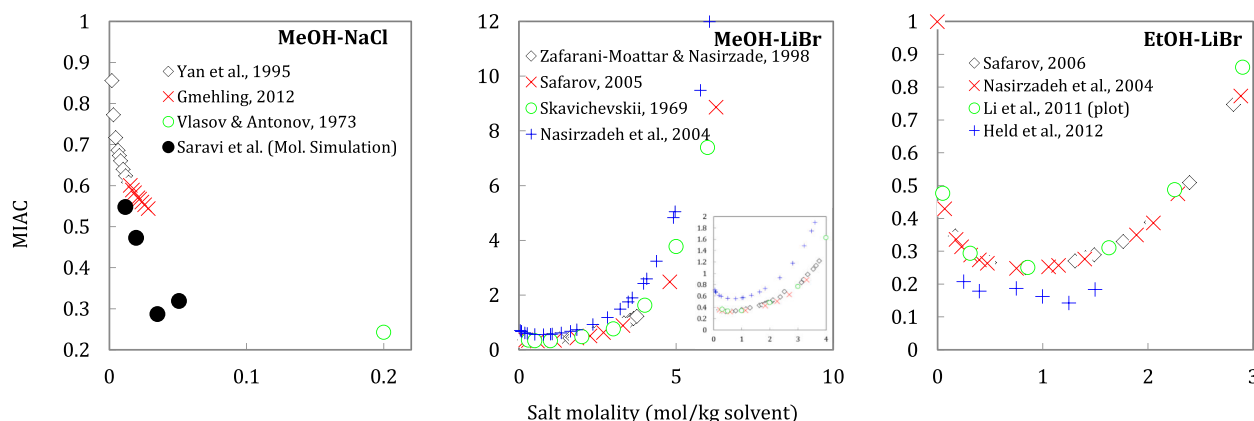


Fig. 1. Comparison of experimental MIAC of NaCl and LiBr in MeOH and LiBr in EtOH. References for the experimental data are shown in Table 4.

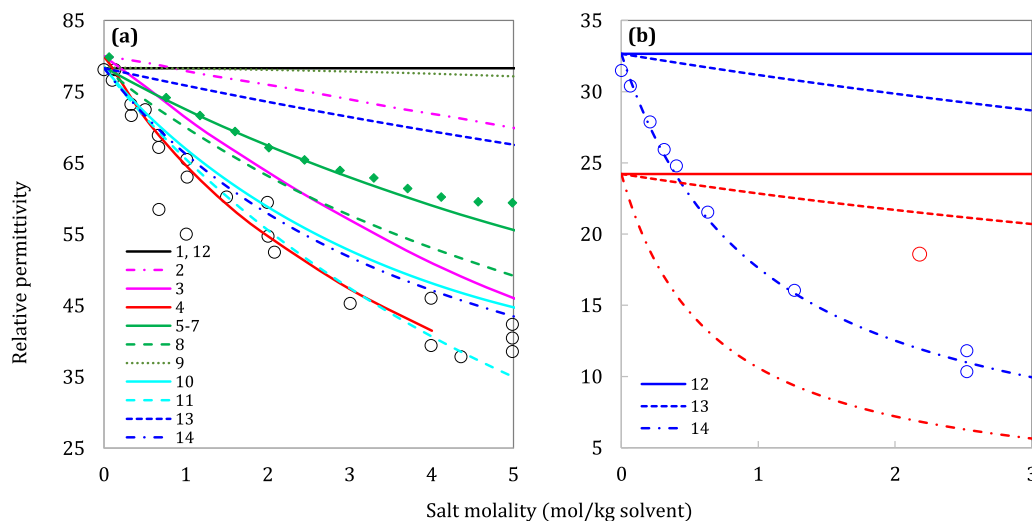


Fig. 2. Relative permittivity of (a) Water-NaCl and (b) MeOH-LiCl and EtOH-LiCl at 298 K and 0.1 MPa. Lines are models (numbers are shown in Table 6), blank points are experimental data, green filled points correspond to kinetic depolarization, reproduced from Maribo-Mogensen et al. [91]. In (b) blue lines and points correspond to MeOH-LiCl and red to EtOH-LiCl.

Table 6

Born and DH contribution in $\ln(\text{MIAC mole fraction scale})$ at molality of 4 mol/kg water for aqueous NaCl solutions at 298.15 K.

Number	Reference	RP model and value at molality of 4 mol/kg water		Born diameter (Å)		Born	DH diameter (Å)		DH
				Na+	Cl-		Na+	Cl-	
1	Walker et al. [9]	Constant	78	-	-	0	2.32	3.34	-0.74
2	Walker et al. [9]	MM ^a for solvent [16]	71	3.36	3.874	0.1	2.32	3.34	-0.84
3	Walker et al. [9]	MM ^a for electrolyte [91]	51	3.36	3.874	1.9	2.32	3.34	-1.62
4	Inchekel et al. [33]	Simonin et al. [92]	42	3.172	4.096	1.2	3.17	4.10	-1.62 ^b
6	Olsen et al. [20] (set 1)	MM ^a for solvent [16]	61	3.33	3.656	0.65	2.36	3.19	-1.10
7	Olsen et al. [20] (set 2)	MM ^a for solvent [16]	61	3.33	3.656	0.65	2.36	3.19	-1.10
8	Olsen et al. [20] (set 3)	MM ^a for solvent [16]	55	3.08	3.98	1	2.63	3.57	-1.30
9	Olsen et al. [20] (set 4)	MM ^a for solvent [16]	78	3.33	3.656	0.1	2.58	3.49	-1.04
10	Valisko and Boda [89]	Polynomial fit of exp data	48	3.24	4.52	1.73 ^c	1.90	3.62	-1.99 ^c
11	Shilov and Lyashchenko [90]	Polynomial fit of exp data	41	-	-	2.18 ^d	-	-	-1.68 ^d
12	This work	Constant	78	-	-	0	1.95	2.94	-0.90
13	This work	MFMR	69	3.36	3.874	0.5	1.95	2.94	-1.15
14	This work	Zuber et al. [32]	48	3.36	3.874	2.46	1.95	2.94	-2.21

^a : MM stands for Maribo-Mogensen et al.

^b : This model utilizes the MSA, not DH term.

^c : This model has no physical interactions and utilizes the adaptive grand canonical Monte Carlo for ion, ion and Born for ion, water interactions.

^d : This model has no physical interactions and utilizes ion-ion and ion-water interactions. Contributions are shown for LiCl and not for NaCl.

their values are entirely predictive. In method II, they kept the ionic diameters the same as in aqueous solutions but fitted the rest of the model parameters to experimental data for ethanol and predicted the rest of the solvents quite well. The latter approach has been further extended by Zuo et al. [39].

Recently, the first predictive approach using transferable parameters between solvents has been presented by Bülow et al. [10]. In this work, the authors claim to have achieved accurate mean ionic activity coefficients (MIAC) and solvation energy predictions using parameters based on aqueous solutions by using a simple, salt-dependent mixing rule to predict the relative permittivity of the electrolyte solutions. In a latter publication, the authors proceeded to model mixed solvent LLE with good results [40]. However, in none of these works the authors show how switching the relative permittivity relation without readjusting the model's parameters affects the MIAC predictions of aqueous solutions and they also do not comment on the physics behind using this particular mixing rule for the relative permittivity. These topics are discussed in this work. Other modeling efforts for single solvent, non-aqueous mixtures are very limited, and most utilize solvent specific ionic diameters fitted to experimental data [41–43].

In recent work on non-aqueous electrolyte solutions, ion pairing has

been included: Müller et al. [44] recently extended the COSMO-RS-ES model to account for ion pairing using the Bjerrum treatment and reported improvement compared to the previous model that did not account for it. On the other hand, Bülow et al. [45] reported that inclusion of the idealized Bjerrum treatment does not significantly affect solubility of salts in organic solvents, unlike the relative permittivity relation, which is crucial. Table 1 is a summary of the discussed models in terms of adjustable parameters, properties used for parameter estimation and relative permittivity.

The importance of the relative permittivity in non-aqueous solutions will be examined in this work, along with the sensitivity of the DH and Born terms to this property, within the context of the eSAFT-VR Mie EoS [27]. This model has been already successfully used for MIAC, density, ion hydration energies [27], gas solubility [28], VLE and LLE of electrolyte solutions [46]. Proper accounting for the dielectric screening of electrolytes is key in modeling electrolyte solutions, however problems arise when we try to define what “accurate dielectric screening” means. Experimentally measured values contain both thermodynamic and kinetic contributions, but should both contributions be used within the EoS framework? Furthermore, ion pairing reduces the decrement of the relative permittivity (RP) compared to free ions. The final goal of this

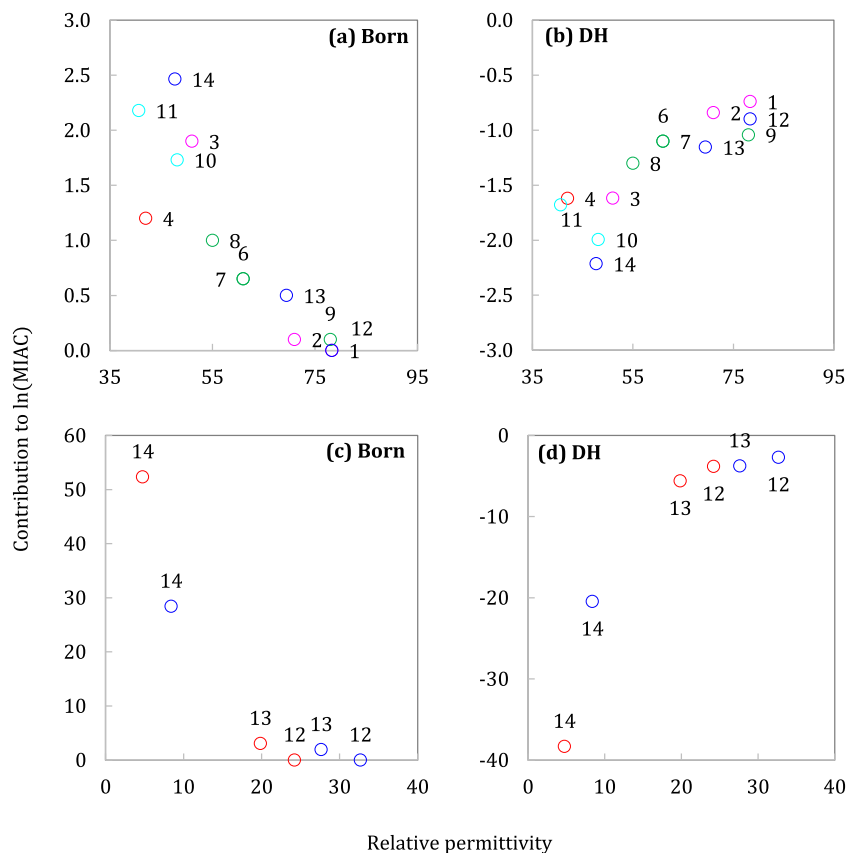


Fig. 3. Contribution of (a, c) Born (or ion, solvent) and (b, d) DH (or ion, ion) terms in $\ln(\text{MIAC})$ vs relative permittivity of (a, b) Water-NaCl and (c, d) MeOH-LiCl (blue) and EtOH-LiCl (red) at 298 K, 0.1 MPa at salt molality 4 mol/kg water. Models numbers as shown in Table 6.

work is to decide which RP relation is more suitable to use in the framework of the eSAFT-VR Mie EoS and will enable us to successfully model non-aqueous solutions. This goal will be approached from an engineering point of view, although some physical explanation for our choice will be provided.

First, an overview of experimental MIAC in non-aqueous solutions is presented, along with a brief evaluation and the database which will be used for validating our model. Afterwards, the effect of the RP in the Born and DH terms will be discussed for aqueous and non-aqueous solutions, both for our own model, as well as models from the literature. The effect of the ion size in the Born and DH terms will also be addressed. Afterwards, eSAFT-VR ionic parameters will be fitted to experimental data of MIAC, individual ion activity coefficient (IIAC), and density of aqueous solutions, using three relations for the RP, with one parameter set per RP relation. In the end, the three versions of the model (one for each RP relation) will be used to predict, without any additional adjustable parameters, MIAC in non-aqueous solutions, and the reason behind the success will be discussed.

2. eSAFT-VR Mie EoS

The physical term of the SAFT-VR Mie EoS [47–49] is extended to electrolyte solutions by adding a DH [17] and a Born [18] term. The different terms will be briefly described in this section.

2.1. SAFT-VR Mie

Within the SAFT framework, associating chain molecules are described as monomer segments with a repulsive core and multiple attractive sites, capable of forming chains and closed rings. These chains are afterwards allowed to form hydrogen bonds at specific associating

sites. Using the common nomenclature of SAFT-type models, the Helmholtz free energy of SAFT-VR Mie (and of most SAFT models) is calculated according to the expression Eq. (1):

$$a^{\text{residual}} = a^{\text{monomer}} + a^{\text{chain}} + a^{\text{association}} \quad (1)$$

$$\text{where } a = \frac{A}{Nk_B T}$$

In this model, the assumed interaction potential between two spherical segments of diameter σ , whose centers are at distance r , is the Mie potential, shown in Eq. 2. This is a generalized Lennard-Jones (LJ) potential with varying repulsive and attractive exponents, λ_r and λ_a , and potential energy depth, ϵ :

$$u^{\text{Mie}}(r) = C\epsilon \left[\left(\frac{\sigma}{r} \right)^{\lambda_r} - \left(\frac{\sigma}{r} \right)^{\lambda_a} \right] \quad (2)$$

where the pre-factor C is given by Eq. 3.

$$C = \frac{\lambda_r}{\lambda_r - \lambda_a} \left(\frac{\lambda_r}{\lambda_a} \right)^{\frac{\lambda_a}{\lambda_r - \lambda_a}} \quad (3)$$

The monomer or segment term incorporates the free energy due to repulsive and dispersion interactions; the latter ones are expanded in series around an effective hard sphere reference fluid. In SAFT-VR Mie, the expansion is truncated to the third order Eq. (4):

$$a^{\text{monomer}} = m_s (a^{\text{hard sphere}} + \beta a_1 + \beta^2 a_2 + \beta^3 a_3) \quad (4)$$

where $\beta = 1/(k_B T)$, a_1 , a_2 , a_3 are the perturbation coefficients and m_s is the segment number.

Monomers are bonded at distance σ from their centers, which is the segment diameter, to form chains. The term corresponding to chain formation is expressed as Eq. (5):

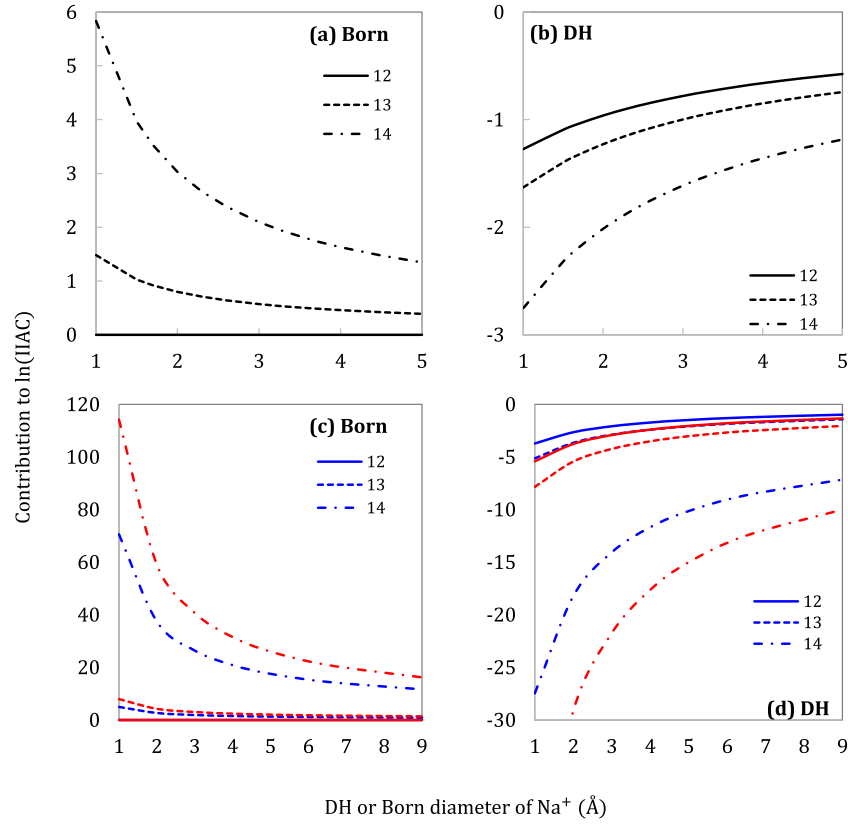


Fig. 4. Contribution of (a, c) Born and (b, d) DH terms in $\ln(\text{IAC})$ of the cation) vs characteristic ionic diameter of the cation in (a, b) Water-NaCl, (c, d) MeOH-LiCl (blue) and EtOH-LiCl (red) at 298 K and 0.1 MPa and salt molality 4 mol/kg water. Models numbers as shown in Table 6.

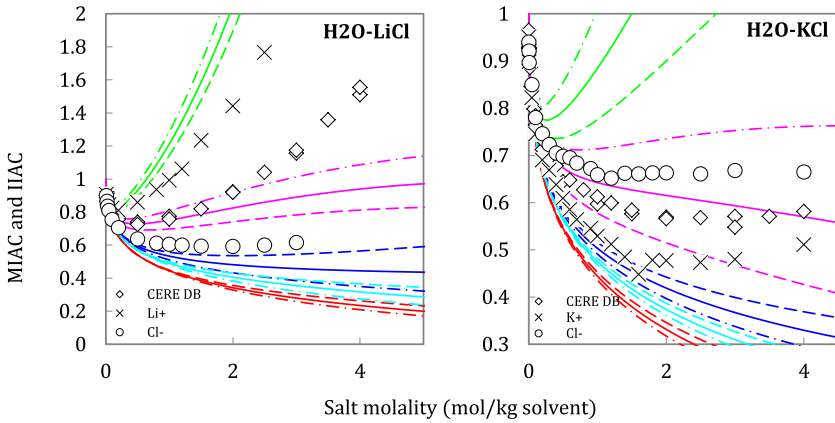


Fig. 5. MIAC and IAC in aqueous solutions with the eSAFT-VR Mie EoS using different approaches for the relative permittivity in a predictive manner. Points are experimental MIAC data from the CERE database[83] or IAC from Wilczek-Vera et al. [96]. Lines are model predictions: solid lines correspond to MIAC, dashed lines to cation IAC and dashed-dot lines to anion IAC. Red lines correspond to the constant relative permittivity, blue to the MFMR, HS; light blue to MFMR, RH; green to Zuber et al., HS; and pink to Zuber et al., RH. RH stands for Born diameters by Rashin and Honig [53], HS stands for Born diameters assumed equal to hard sphere diameters of the ions.

$$a^{\text{chain}} = -(m_s - 1) \ln g^{\text{Mie}}(\sigma) \quad (5)$$

where $g^{\text{Mie}}(\sigma)$ is the radial distribution function at contact.

A consistent association term, which can be found in the work of Dufal et al. [48], complements the SAFT-VR Mie EoS for associating chains of Mie segments with s bonding site types, n_a sites of type a , $a = 1, \dots, s$, obtained from Eq. 6–9:

$$a^{\text{association}} = \sum_{a=1}^s n_a \left(\ln X_a - \frac{1}{2} X_a + \frac{1}{2} \right) \quad (6)$$

where X_a is the fraction of molecules not bonded at sites of type a found from the following relation:

$$1 = X_a + \rho X_a \sum_{b=1}^s n_b X_b \Delta_{ab} \quad a = 1, 2, \dots, s. \quad (7)$$

Δ_{ab} characterizes the strength and bonding volume of the association interaction between two associating sites a and b , and is given by:

$$\Delta_{ab} = F_{ab} K_{ab} I \quad (8)$$

where F_{ab} is the Mayer function and I the association kernel:

$$F_{ab} = \exp(\beta \epsilon_{ab}^{\text{HB}}) - 1 \quad (9)$$

where $\epsilon_{ab}^{\text{HB}}$ represents the depth of the square well potential used to describe the association site.

The complete set of the model's equations can be found in the

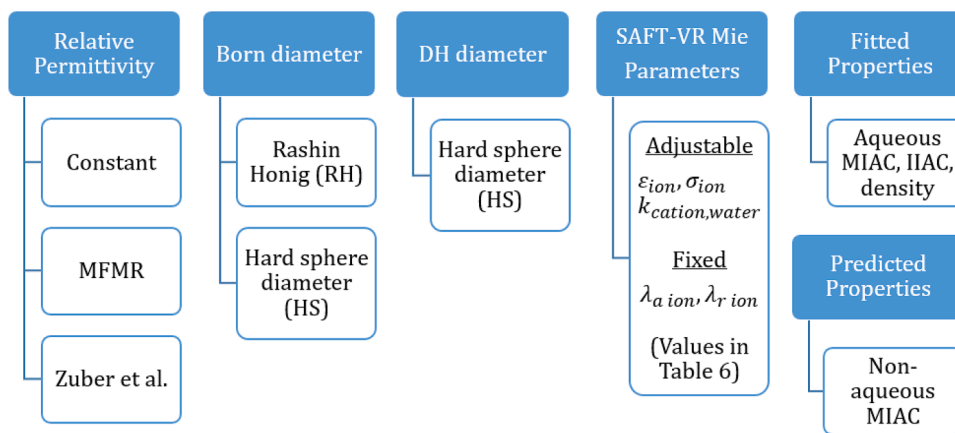


Fig. 6. Schematic representation of the modeling approach used in this work.

original SAFT-VR Mie publications [47–49]. SAFT-VR Mie model utilizes five adjustable parameters per component, namely the segment number, m , the segment diameter, σ , the dispersion energy, ϵ/k_B , the repulsive, λ_r , and attractive, λ_a , exponents of the Mie potential (although the attractive exponent is usually used as a constant equal to 6). For associating compounds, two additional parameters are required, namely the association energy, ϵ_{ab}^{HB}/k_B and the association volume, K_{ab} .

Extension to mixtures requires mixing rules for the dispersion term along with suitable combining rules, shown in Eq. 10–16, to take into account that the mixtures are non-conformal:

$$m_s = \sum_{i=1}^{Components} x_i m_i \quad (10)$$

$$n_a = \sum_{i=1}^{Components} x_i n_{ai} \quad (11)$$

where x_i is the mole fraction of component i , m_i is the segment number of component i , and n_{ai} is the number of sites of type a in molecule i .

The unlike parameters between components i and j are determined as:

$$\epsilon_{ij} = \sqrt{\epsilon_{ii}\epsilon_{jj}} \frac{\sqrt{\sigma_{ii}^3\sigma_{jj}^3}}{\sigma_{ij}^3} (1 - k_{ij}) \quad (12)$$

$$\sigma_{ij} = \frac{\sigma_{ii} + \sigma_{jj}}{2} \quad (13)$$

$$\lambda_{k,ij} - 3 = \sqrt{(\lambda_{k,ii} - 3)(\lambda_{k,jj} - 3)} \quad (14)$$

$$\epsilon_{abij}^{HB} = \sqrt{\epsilon_{abii}^{HB}\epsilon_{abjj}^{HB}} \quad (15)$$

$$K_{abij} = \left(\frac{\sqrt[3]{K_{abii}} + \sqrt[3]{K_{abjj}}}{2} \right)^3 \quad (16)$$

where σ_{ii} is the segment diameter of component i , ϵ_{ii} is the dispersion energy of i , k_{ij} is a binary interaction parameter, $\lambda_{k,ii}$ is the repulsive ($\lambda_{r,ii}$) or attractive ($\lambda_{a,ii}$) exponent of the Mie potential of component i , ϵ_{abii}^{HB} is the association energy and K_{abii} the bonding volume of component i .

In the framework of the eSAFT-VR Mie model [27,28], the dispersion energy between like and unlike ions is calculated through Eq. 17, which is obtained from equating the London dispersion interaction potential to the attractive part of the Lennard-Jones potential, similar to the methodology of the Hudson-McCoubrey combining rule [50], as presented by Haslam et al. [51]:

$$\epsilon_{ij} = \frac{3}{8} \frac{1}{\sigma_{ij}^6} \frac{a_{0,i}a_{0,j}}{(4\pi\epsilon_0)^2} \frac{I_i I_j}{(I_i + I_j)} \quad (17)$$

where $a_{0,i}$ is the electronic polarizability of component i and I_i the ionization potential.

2.2. Debye – Hückel term

To account for the long-range, electrostatic interactions between ions, the DH theory is used. According to this approach, the Helmholtz free energy contribution due to ion-ion electrostatic interactions is calculated from Eqs. 18–20 [17,52]:

$$a^{DH} = -\frac{1}{4\pi\epsilon_0\epsilon_r} \sum_{i=1}^{NIONS} x_i Z_i^2 \frac{\kappa}{3} \chi(\kappa d_i) \quad (18)$$

$$\kappa = \sqrt{\frac{e^2}{\epsilon_0\epsilon_r} \frac{N_A}{k_B T} \frac{\sum_{i=1}^{NIONS} x_i Z_i^2}{v}} \quad (19)$$

$$\chi(y) = \frac{3}{y^3} \left(\frac{3}{2} + \ln(1+y) - 2(1+y) + \frac{1}{2}(1+y)^2 \right) \quad (20)$$

where x_i is the mole fraction of ion i , Z_i is its valence and d_i is its characteristic diameter or distance of closest approach, κ is the inverse Debye screening length, χ is a function of $y = \kappa d_i$, e is the elementary charge, ϵ_0 is the permittivity in vacuum and ϵ_r is the relative permittivity (or dielectric constant) of the solution, T is temperature, v is the molar volume, and k_B is the Boltzmann constant. In our implementation, the DH characteristic diameter is taken to be the hard sphere diameter of the ionic species which is calculated according the Barker-Henderson expression [27,47].

2.3. Born term

The Born term [18,52] accounts for the energy needed to transfer an ion from vacuum to a dielectric medium (Eq. 21):

$$a^{Born} = \frac{e^2 N_A}{4\pi\epsilon_0} \left(\frac{1}{\epsilon_r} - 1 \right) \sum_{i=1}^{NIONS} \frac{x_i Z_i^2}{d_i^{Born}} \quad (21)$$

where d_i^{Born} is the diameter of the cavity occupied by ion i in the solvent. The Born diameter is taken from the work of Rashin and Honig [53] which is abbreviated as RH within this work.

2.4. Relative permittivity of pure solvents

The dielectric constant or relative permittivity of the solvents used in

Table 7

eSAFT-VR Mie fitted ionic parameters using different relative permittivity relations and different Born term diameter for aqueous solutions.

	$\epsilon_{\text{ion}}/k_B$ (K)	$\epsilon_{\text{ion,water}}/k_B$ (K)	$k_{\text{ion,water}}$	σ_{ion} (Å)
Constant RP (Selam et al. [27])^a				
Li+	3.00	893.71	-26.4905	1.8942
Na+	32.40	187.62	-0.6862	2.1607
K+	144.15	68.40	0.7190	2.6273
Cl-	118.67	594.05	-1.6675	3.0999
Br-	92.36	543.53	-1.7845	3.4887
I-	97.28	522.56	-1.6481	3.8870
Constant RP, This work^{b, g}				
Li+	234.64	828.56	-1.6552	2.7700
Na+	416.14	1058.41	-1.7597	1.9000
K+	1107.73	846.32		2.8000
Cl-	59.91	594.05	0.0000	3.0800
Br-	223.29	543.53	0.0000	3.3000
I-	264.73	522.56	0.0000	3.7000
MFMR, HS^{c, g}				
Li+	201.53	755.69	-1.6329	2.5709
Na+	584.15	782.53	-0.6507	2.1893
K+	1316.61	893.46	-0.2087	2.7711
Cl-	86.46	190.09	0.0000	3.0259
Br-	259.22	326.71	0.0000	3.5198
I-	261.32	324.10	0.0000	3.8401
MFMR, RH^{d, g}				
Li+	132.50	769.95	-2.2948	2.6642
Na+	613.48	817.54	-0.6342	2.5514
K+	1651.77	1037.50	-0.2593	3.5531
Cl-	110.61	214.58	0.0000	2.8388
Br-	227.76	308.52	0.0000	3.1026
I-	314.97	359.78	0.0000	3.5507
Zuber et al., HS^{e, g}				
Li+	240.64	298.56	-0.0136	1.9566
Na+	568.14	447.41	0.0756	2.6697
K+	1173.73	630.32	0.0998	3.1536
Cl-	89.91	188.09	0.0000	4.0610
Br-	205.29	285.27	0.0000	3.9879
I-	341.73	372.31	0.0000	3.7333
Zuber et al., RH^{f, g}				
Li+	146.48	421.80	-0.7112	2.7609
Na+	435.11	519.96	-0.2903	2.0687
K+	1151.50	676.62	0.0242	3.1703
Cl-	96.53	195.41	0.0000	4.0093
Br-	156.51	251.10	0.0000	3.8155
I-	310.67	356.84	0.0000	3.5926

^a : Model of Selam et al. [27], utilizing a constant relative permittivity (RP), equal to that of the solvent.

^b : Determined in this work with a constant RP. The major difference with the Selam model is the inclusion of IAC in the parameterization.

^c MFMR, HS: Mole fraction mixing rule (MFMR) for the RP and Born diameter equal to Hard Sphere diameter.

^d MFMR, RH: MFMR for the RP and Born diameter from Rashin and Honig [53].

^e Zuber et al., HS: Zuber et al. for the RP and Born diameter equal to Hard Sphere diameter.

^f Zuber et al., RH: Zuber et al. for the RP and Born diameter from Rashin and Honig [53].

^g : $\epsilon_{\text{anion,water}}$ is determined from combining rule (Eq. 12).

this work are presented in Table 2. They are taken from the work of Zuo and Furst [38] and are temperature dependent.

Within the framework of eSAFT-VR Mie, up until now the relative permittivity of the solution was equal to that of the solvent medium, and the salt concentration did not have any impact value of the relative permittivity of the solution. In this work, this will be challenged. More details are given in “Section 3.2. Relative permittivity of electrolyte solutions”.

2.5. Pure component parameter for solvents

The pure component parameters for the solvents used in this work

are presented in Table 3. No pure component parameters for ethanol are available in the literature for SAFT-VR Mie, so they were estimated in this work.

3. Results and discussion

3.1. Evaluation of experimental MIAC measurements in non-aqueous electrolyte solutions

MIAC (in the molality scale unless otherwise mentioned) can be determined from potentiometric data, as long as the standard potential of the cell is known, and solvent activity data, which can be converted to MIAC by utilizing fundamental equations. Solvent activity can be determined by freezing point depression, boiling point elevation and vapor pressure measurements of the electrolyte solutions [54]. The solubility product of single salts can be converted to MIAC values, assuming that the solid phase that precipitates is pure salt [55]. Such data are difficult to find in the literature, unlike vapor pressure and osmotic coefficient measurements that are more common.

The majority of vapor pressure measurements in the literature are isopiestic measurements, which are usually more accurate at molality higher than 0.1 molal [54]. The conversion of vapor pressure to osmotic coefficients and vice versa is rather straight forward; the vapor phase consists only of solvent molecules and it can either be considered ideal at ambient conditions or a virial type equation may be used [56]. On the other hand, while converting the osmotic coefficients to activity coefficients caution should be exercised. To calculate MIAC from osmotic coefficients the Gibbs-Duhem relation is used and a graphical integration of the osmotic coefficient with molality is performed. However, an accurate estimate of the dilute region osmotic coefficients is necessary, which is usually calculated by a thermodynamic model [54]. Recently, Passamonti et al. [57] discussed how to consistently transform osmotic coefficients to MIAC data.

Barthel et al. [56,58,59] use for this purpose the Pitzer model. As an alternative, a model can be fitted to osmotic coefficient data, and then used to predict MIAC, skipping the Gibbs-Duhem equation. In latter publications, Barthel et al. used the osmotic coefficients to fit the parameters of the Pitzer model, which is afterwards used to predict activity coefficients [60–62]. Nasirzadeh et al. [63–66] followed a similar approach using the Pitzer equation with the Archer extension and other models. In our work, when multiple models have been used for this purpose and different sets of MIAC are reported in the same paper, we have used the average of the activity coefficients. Safarov [67–69] and Xin et al. [8] utilized for the same purpose the Archer extension of the Pitzer-Mayorga model, while Zafarani-Moatari et al. used the Pitzer and Clegg-Pitzer models [70]. Held et al. [42] used a power series to model the osmotic coefficient and obtained the activity coefficient by means of Gibbs-Duhem although nothing is mentioned about how they handled the dilute region. Skabichevskii [71] reports a graphical integration also without any mention of the dilute region.

Table 4 shows a summary of experimental MIAC data for non-aqueous solutions of single salts found in the literature. Most of the data represent lithium salts due to their large solubility values in non-aqueous solvents. These systems are also currently of great importance mostly due to the lithium battery industry [8]. Sodium and potassium salts have very low solubility in alcohols and they are mostly measured by potentiometric methods.

For a few systems, more than one set of experimental data have been reported and, for even fewer systems, evaluation of the datasets is possible. Plots comparing the different datasets can be found in the Supplementary Material. Three datasets have been excluded from this work as they were found inconsistent with other datasets, as shown in Fig. 1. For NaCl in methanol, the point from Vlasov and Antonov [78] has been excluded as it is reported for higher salt solubility than the experimentally measured. In this plot, the molecular simulation data produced by Saravi et al. [82] are also shown, although they are not used

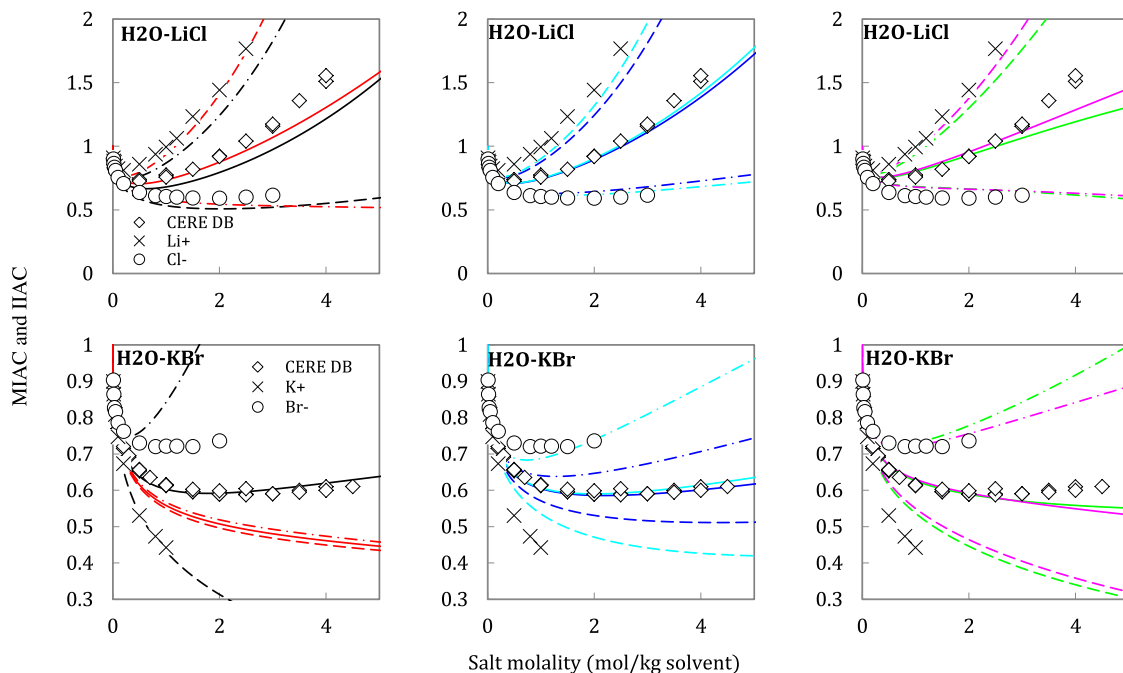


Fig. 7. MIAC and IIAC in aqueous solutions with the eSAFT-VR Mie EoS using different approaches for the relative permittivity and the parameters of Table 7. Points are experimental MIAC [83] or IIAC [96] data. Lines are model predictions: solid lines correspond to MIAC, dashed lines to cation IIAC and dashed-dot lines to anion IIAC. Black: model of Selam et al. [27], utilizing a constant relative permittivity (RP); red: this work using a constant RP; blue: MFMR, HS: Mole fraction mixing rule (MFMR) for the RP and Born diameter equal to Hard Sphere (HS) diameter; light blue: MFMR, RH: MFMR for the RP and Born diameter from Rashin and Honig (RH) [53]; green: Zuber et al., HS: Zuber et al. for the RP and Born diameter equal to HS diameter; pink: Zuber et al., RH: Zuber et al. for the RP and Born diameter from RH.

further in this work. The data of Held et al. [42] report lower MIAC of LiBr in ethanol (Fig. 1), which have been excluded as they disagree with three other datasets. The data by Nazirzadeh [63] for LiBr in methanol (Fig. 1) also disagree with three other datasets and will therefore not be considered in this work. There are also two datasets for LiBr in 2-propanol [65,70], which agree very well with each other. The final database used in this work is presented in Table 5.

3.2. Relative permittivity of electrolyte solutions

The importance of the relative permittivity for electrolyte EoS has been explained in the introduction, along with the different approaches for its determination in the framework of EoS modeling. Due to this high importance, we investigated its effect in the contribution magnitude of the different electrolyte terms. We have collected data from literature studies where a relative permittivity plot is presented along with a plot analysing the contribution of electrolyte terms, DH or MSA and Born, in the rational MIAC and added some calculations of our own. A comparison is made in terms of relative permittivity in Fig. 2 and in terms of the contribution of different terms at a molality of salt equal to 4 mol/kg in Fig. 3 and Table 6. The literature values have been read from plots so there is some uncertainty in the values reported in Table 6.

Bülöw et al. [10,45,87] utilized a salt-concentration dependent relative permittivity in their most recent version of the ePC-SAFT EoS. More specifically, they used a simple mixing rule to predict the relative permittivity of mixtures, which is a good approximation of the experimental relative permittivity of ionic liquids-water solutions [87]:

$$\epsilon_r^{\text{mix}} = \sum_{i=1}^{\text{solvents+ions}} x_i \epsilon_r^{\text{pure}, i} \quad (22)$$

where x_i is the mole fraction of component i , and $\epsilon_r^{\text{pure}, i}$ is the relative permittivity of pure component or ion i . For ionic liquids $\epsilon_r^{\text{pure}, i} = 12$

[87], however, in a later work, they switched to $\epsilon_r^{\text{pure}, i} = 8$ for strong electrolyte solutions [10], an approximation of salt relative permittivity data [88]. In our work we used this value for all ions, $\epsilon_r^{\text{ion}} = 8$, and from now on we will refer to this mixing rule as Mole Fraction Mixing Rule (MFMR). As shown in our previous work [46], the MFMR is not very accurate at predicting the relative permittivity of mixed solvents (alcohol - water) therefore the MFMR will be combined with a volume fraction based mixing rule for mixed solvent predictions in our subsequent work.

Last but not least, we will use another relation for the calculation of the relative permittivity of electrolyte solutions, proposed by Zuber et al. [32]

$$\epsilon_r^{\text{mix}} = \frac{\epsilon_r^{\text{mix, non-electrolyte}}}{1 + \sum_{i=1}^{\text{ions}} x_i \sum_{j=1}^{\text{solvent}} a_{ij} \varphi_j} \quad (23)$$

where $\epsilon_r^{\text{mix, non-electrolyte}}$ is the relative permittivity of the single or mixed solvent without the salt, a_{ij} is the adjustable parameter of ion i in solvent j , and φ_j is a parameter calculated on an ion-free basis. The general parameters a_{ij} tabulated in Table 9 of the original article [32] have been used in this work: a single value is used for all cations and another one for all anions per solvent. This relation was fitted to experimental data, therefore it also includes the kinetic part of the relative permittivity. As discussed in the introduction, it may not be correct to use both the thermodynamic and kinetic contributions in EoS modeling.

The aforementioned relations for the relative permittivity along with some taken from the literature are plotted in Fig. 2 for NaCl in water at 298.15 K and 0.1 MPa. The MFMR (model 13) exhibits a great similarity with the Maribo-Mogensen solvent model as implemented by Walker et al. [9] (model 2) and they seem to yield the same relative permittivity if the intercept of the two models (pure water relative permittivity is constant) are the same. The Maribo-Mogensen model for solvent relative permittivity within the eCPA framework (models 5-9) yields

Table 8

AARD%^a in MIAC, IIAC and density (ρ) for aqueous solutions with eSAFT-VR Mie fitted ionic parameters presented in Table 7.

	MIAC	Cation IIAC	Anion IIAC	ρ
Constant RP (Selam et al. [27])^b				
LiCl	10.9	34.4	49.8	0.4
LiBr	2.9	28.0	53.6	2.3
LiI	5.2	-	-	2.4
NaCl	2.4	30.8	42.4	0.7
NaBr	3.2	30.3	59.8	5.8
NaI	3.0	-	-	1.9
KCl	2.2	16.3	24.2	0.9
KBr	1.8	1.5	12.3	0.6
KI	2.2	-	-	2.5
Total	3.7	23.6	40.3	1.9
Constant RP, This work^{c, h}				
LiCl	5.4	3.7	4.0	2.8
LiBr	3.6	14.5	9.4	1.2
LiI	2.4	-	-	1.3
NaCl	6.1	12.2	2.7	0.9
NaBr	2.7	5.4	3.1	5.9
NaI	2.8	-	-	3.2
KCl	5.8	3.6	14.1	1.2
KBr	11.2	7.0	12.4	0.9
KI	7.7	-	-	3.4
Total	5.3	7.7	7.6	2.3
MFMR, HS^{d, h}				
LiCl	3.6	8.9	3.9	2.2
LiBr	4.2	10.4	5.1	1.3
LiI	5.5	-	-	1.1
NaCl	4.6	6.6	2.3	0.5
NaBr	2.6	2.3	3.4	4.4
NaI	4.6	-	-	1.9
KCl	2.0	3.4	4.1	1.5
KBr	1.1	8.5	6.4	0.5
KI	2.5	-	-	1.8
Total	3.4	6.7	4.2	1.7
MFMR, RH^{e, h}				
LiCl	2.8	6.6	2.0	1.7
LiBr	2.7	9.2	7.2	2.0
LiI	2.5	-	-	2.0
NaCl	3.7	5.9	1.5	0.6
NaBr	3.3	2.6	4.7	5.2
NaI	2.6	-	-	2.4
KCl	2.1	4.3	4.9	0.8
KBr	1.1	6.3	2.5	0.5
KI	2.1	-	-	0.5
Total	2.6	5.8	3.8	1.7
Zuber et al., HS^{f, h}				
LiCl	5.8	6.2	7.4	7.9
LiBr	5.0	6.1	4.6	2.1
LiI	2.7	-	-	2.3
NaCl	4.9	5.3	5.8	6.9
NaBr	7.1	5.3	7.1	1.3
NaI	3.1	-	-	1.1
KCl	2.5	7.2	2.0	4.2
KBr	2.4	7.0	1.9	2.8
KI	2.3	-	-	2.3
Total	4.0	6.2	4.8	3.4
Zuber et al., RH^{g, h}				
LiCl	4.9	3.6	7.2	9.3
LiBr	5.1	6.7	2.1	2.7
LiI	1.6	-	-	1.2
NaCl	5.9	5.7	6.6	5.1
NaBr	8.1	4.8	7.4	3.1
NaI	0.4	-	-	2.8
KCl	2.7	7.8	2.4	4.0
KBr	2.8	7.9	1.2	2.2
KI	7.2	-	-	0.4
Total	4.3	6.1	4.5	3.4

$$^a : \text{AARD\%} = \frac{100}{NP} \sum_1^{NP} \left(\left| \frac{x^{exp} - x^{calc}}{x^{exp}} \right| \right).$$

^b : Model of Selam et al. [27], utilizing a constant relative permittivity (RP), equal to that of the solvent.

^c : Determined in this work with a constant RP. The major difference with the Selam model is the inclusion of IIAC in the parameterization.

^d : MFMR, HS: Mole fraction mixing rule (MFMR) for the RP and Born diameter equal to Hard Sphere diameter.

^e : MFMR, RH: MFMR for the RP and Born diameter from Rashin and Honig [53].

^f : Zuber et al., HS: Zuber et al. for the RP and Born diameter equal to Hard Sphere diameter.

^g : Zuber et al., RH: Zuber et al. for the RP and Born diameter from Rashin and Honig [53].

^h : $\epsilon_{anion, water}$ is determined from combining rule (Eq. 12).

significantly different values for the relative permittivity as a result of the different parameterizations of eCPA. The different parameters result in different mixture density and, consequently, different relative permittivity predictions. The models used in the work of Inchekele et al. [33] (model 4) and Zuber et al. [32] (model 14) reproduce the experimental data accurately, similar to those by Valisko and Boda [89] (model 10) and Shilov and Lyashchenko [90] (model 11).

To investigate the effect of the relative permittivity in the various electrolyte terms we calculated the Born and DH contributions to the rational, asymmetric MIAC using the aforementioned relative permittivity relations along with their full compositional derivatives. The values of the contributions of the electrolyte terms in the rational MIAC are shown in Table 6 for a NaCl molality equal to 4 mol/kg water. The same values are plotted in Fig. 3.

Apart from the relative permittivity and its derivatives, the other parameters entering the two electrolyte terms are the characteristic ionic diameters, which are different for the DH and Born terms. Common approaches for the DH or MSA ionic diameters include assuming that they are equal to the bare ion diameters determined by crystallographic [31] or other experimental data [93], or are fitted parameters within the EoS framework [15,27,33,36,94,95]. In many EoS, the DH or MSA ionic diameters are assumed equal to the hard sphere diameter of the ions [27, 31,34], or related to them using a fixed ratio [36]. The Born diameters on the other hand are a bit more freely chosen: some assume that they are also equal to the DH or MSA diameters [10,34,94] or the hard sphere diameters [15], while others fit them to hydration enthalpies [27,31,36, 93], or directly to other properties within the EoS framework [33].

The influence of the selected ionic diameters in the two electrolyte terms within the eSAFT-VR Mie framework is shown in Fig. 4. Fig. 3 and Fig. 4 demonstrate that the sensitivity of the Born term contribution to the Individual Ion Activity Coefficient (IIAC) with respect to the characteristic diameter and the relative permittivity is more significant than that of the DH term and that both terms become more sensitive at small characteristic diameters. For the Zuber et al. relation (model 14), both terms have significantly higher contributions compared to the MFMR (model 13), meaning that as the salt concentration dependence of the relative permittivity increases, so does its effect on the electrolyte terms.

The relative permittivity of LiCl in methanol and ethanol is shown in Fig. 2 and its effect on the Born and DH terms in Fig. 3. In Fig. 4, the effect of the characteristic diameter in the electrostatic terms is shown. From both plots it can be concluded that the contribution of both electrolyte terms scale very rapidly with relative permittivity, and even more so with the characteristic diameter. These observations are similar to aqueous solutions; here, however, the effect is much larger, leading to an order of magnitude greater Born and DH contributions. It seems that in order to get reasonable Born and DH contributions in MIAC from a mathematical point of view, one can choose either a small contribution of the salt in the solution relative permittivity or a larger characteristic diameter in the electrostatic terms; these two modeling components have similar effects.

3.3. eSAFT-VR Mie modeling of aqueous systems

The MIAC in aqueous solutions have been correlated with eSAFT-VR

Table 9AARD%^a in MIAC of single salts in single solvents at 298.15 K and atmospheric pressure.

System	Selam et al. ^b	Constant RP ^{c, h}	MFMR, HS ^{d, h}	MFMR, RH ^{e, h}	Zuber et al., HS ^{f, h}	Zuber et al., RH ^{g, h}
LiCl in H2O	10.9	5.4	3.6	2.8	5.8	4.7
LiCl in MeOH	55.0	42.0	10.2	20.4	>100	>100
LiCl in EtOH	50.6	37.7	10.3	18.8	>100	>100
LiBr in H2O	2.9	3.6	4.2	2.7	5.0	10.3
LiBr in MeOH	53.5	42.8	13.9	23.0	>100	>100
LiBr in EtOH	67.7	57.0	23.4	37.9	>100	>100
LiI in H2O	5.2	2.4	5.5	2.5	2.7	12.5
LiI in MeOH	20.9	15.4	8.4	10.6	>100	>100
LiI in EtOH	48.5	30.8	10.7	6.2	>100	>100
NaCl in H2O	2.4	6.1	4.6	3.7	4.9	24.4
NaCl in MeOH	9.3	9.1	10.1	10.0	23.5	20.9
NaCl in EtOH	10.6	11.0	9.0	9.2	42.7	28.3
NaBr in H2O	3.2	2.7	2.6	3.3	7.1	8.8
NaBr in MeOH	24.3	28.2	10.9	17.1	>100	>100
NaBr in EtOH	10.6	12.1	4.5	6.3	>100	>100
NaI in H2O	3.0	2.8	4.6	2.6	3.1	0.4
NaI in MeOH	21.0	23.6	14.9	17.3	>100	>100
NaI in EtOH	39.9	44.7	18.6	29.0	>100	>100
KCl in H2O	2.2	5.8	2.0	2.1	2.5	5.0
KCl in MeOH	4.5	4.3	5.9	5.3	42.3	30.3
KBr in H2O	1.8	11.2	1.1	1.1	2.4	2.9
KBr in MeOH	20.0	20.9	18.0	19.9	46.7	22.8
KI in H2O	2.2	7.7	2.5	2.1	2.3	6.0
KI in MeOH	13.8	14.2	13.7	14.5	>100	41.2
AARD% in all solvents	23.8	21.4	8.6	12.4	>100	>100
AARD% in H2O	3.4	5.5	3.2	2.7	4.3	4.8
AARD% in MeOH	35.8	29.9	11.0	17.1	>100	>100
AARD% in EtOH	40.6	35.5	13.7	21.4	>100	>100

$$^a : \text{AARD\%} = \frac{100}{NDP} \sum_1^{NDP} \left(\left| \frac{\gamma_{\pm}^{exp} - \gamma_{\pm}^{calc}}{\gamma_{\pm}^{exp}} \right| \right).$$

^b : Model of Selam et al. [27], utilizing a constant relative permittivity (RP), equal to that of the solvent.

^c : Determined in this work with a constant RP.

^d : MFMR, HS: Mole fraction mixing rule (MFMR) for the RP and Born diameter equal to Hard Sphere diameter.

^e : MFMR, RH: MFMR for the RP and Born diameter from Rashin and Honig[53].

^f : Zuber et al., HS: Zuber et al. for the RP and Born diameter equal to Hard Sphere diameter.

^g : Zuber et al., RH: Zuber et al. for the RP and Born diameter from Rashin and Honig[53].

^h : $\epsilon_{anion,water}$ is determined from combining rule (Eq. 12).

Mie using different relations for the relative permittivity. The constant relative permittivity has been utilized along with the MFMR (Eq. 22) and the Zuber correlation (Eq. 23). These three approaches for the relative permittivity will be compared in the framework of eSAFT-VR Mie for aqueous solutions. First, to get a measure of the effect of the relative permittivity, a plot of the prediction of MIAC and IAC is presented in Fig. 5. In this predictive approach, the ionic parameters (ϵ_{ion} and σ_{ion}) by Selam et al. [27] have been retained while the unlike interactions are determined through the eSAFT-VR Mie combining rules with zero binary interaction parameters.

It is shown that the relative permittivity plays a huge role in the prediction of MIAC and IAC, even for aqueous electrolyte solutions. From a first glance, the Zuber et al. relation with the Born diameters of Rashin and Honig [53] seems to be rather accurate for both salts, but a more careful examination reveals that the trend in IAC is wrong for LiCl: Li+ is predicted lower than Cl-, while experimental values suggest otherwise. The same happens also for NaCl. The experimental trend is reversed in KCl. All in all, it seems that a) the stronger the effect of the salt in the relative permittivity, the higher the value for the MIAC and IAC and b) the lower the Born diameter of the ion, the larger the IAC.

Due to the huge effect of the relative permittivity, we decided to compare the different relations in a fair manner. For the comparison, the same number of parameters has been fitted to the same database of MIAC, individual ion activity coefficients (IAC) and density of aqueous electrolyte solutions. As in the model by Selam et al. [27], the DH characteristic diameters are assumed equal to the hard sphere diameters

(HS) of eSAFT-VR Mie. The Born diameters on the other hand are allowed to vary: first the Born diameters have also been assumed equal to the HS diameters and also equal to the DH diameters of the ions. Second, they have been assumed equal to the values of Rashin and Honig [53] (RH), as proposed in the work of Selam et al. [27]. This is done for testing whether parameter fitting can conceal the differences between the various relative permittivity relations. For visual guidance, we have included a schematic diagram with our modeling approach, summarizing the RP relations, adjustable parameters, fitted properties, etc (Fig. 6).

In the work of Selam et al.[27], the adjustable parameters per ion were the segment diameter, σ_{ion} , and the ion, water dispersion energy $\epsilon_{ion,water}$. The rest of the ionic parameters, including $\epsilon_{ion,ion}$ between like and unlike ions were determined using a predictive combining rule shown in Eq. 17. Although this approach worked very well for aqueous solutions, we decided to sacrifice it towards having a more predictive model. We chose to fit the pure ion ϵ_{ion} and σ_{ion} and use eSAFT-VR Mie combining rules to determine all the unlike pairs, using Eqs. 12-16. Very quickly, we realized that the determination of the $\epsilon_{anion,water}$ from combining rules worked relatively well for anions, but the same did not happen for cations. If the $\epsilon_{cation,water}$ were not fitted, we could not get a good fit in aqueous solutions with ionic parameters. We chose to fit the binary interaction parameter $k_{cation,water}$ (see Eq. 12) instead to comply with the selected combining rules. The final number of parameters determined per ion are thus 3 for cations (σ_{ion} , ϵ_{ion} , $k_{ion,water}$) and 2 for anions (σ_{ion} , ϵ_{ion}). These parameters were fitted simultaneously for all

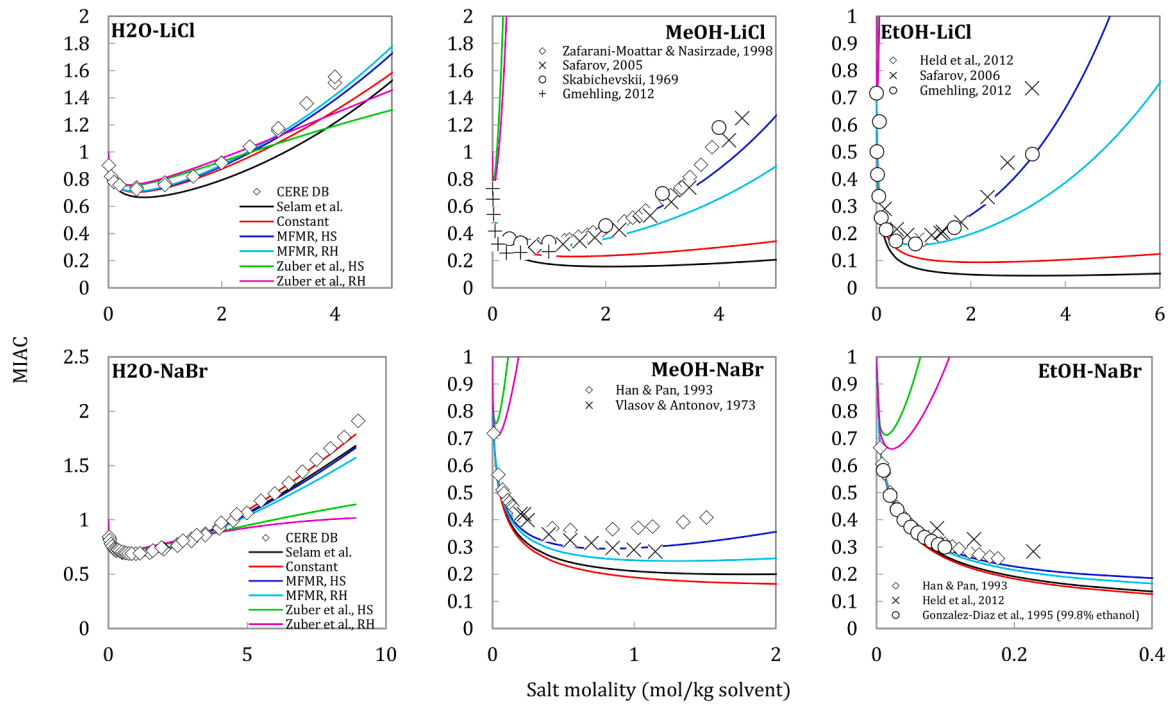


Fig. 8. MIAC in single solvent solutions with the eSAFT-VR Mie EoS using different approaches for the relative permittivity. Points are experimental data (references in Table 5), lines are model predictions. Black: model of Selam et al. [27], utilizing a constant relative permittivity (RP); red: this work using a constant RP; blue: MFMR, HS: Mole fraction mixing rule (MFMR) for the RP and Born diameter equal to Hard Sphere (HS) diameter; light blue: MFMR, RH: MFMR for the RP and Born diameter from Rashin and Honig (RH) [53]; green: Zuber et al., HS: Zuber et al. for the RP and Born diameter equal to HS diameter; pink: Zuber et al., RH: Zuber et al. for the RP and Born diameter from RH.

Table 10

Extension of eSAFT-VR Mie Selam et al. [27] model to different solvents. The segment diameter, σ_{ion} was kept the same as in Table 7.

	$\epsilon_{ion,MeOH}/k_B$ (K)	$\epsilon_{ion,EtOH}/k_B$ (K)
Li+	3102.43	3814.62
Na+	1882.94	1382.41
K+	1386.11	-
Cl-	597.99	452.42
Br-	165.95	792.21
I-	312.89	635.50

ions based on the following objective function (Eq. 24):

$$\begin{aligned}
 F = & \frac{2}{NP_{MIAC}} \sum_i^{NP_{MIAC}} \left(\left| \frac{MIAC^{exp} - MIAC^{calc}}{MIAC^{exp}} \right| \right) \\
 & + \frac{2}{NP_{\rho}} \sum_i^{NP_{\rho}} \left(\left| \frac{\rho^{exp} - \rho^{calc}}{\rho^{exp}} \right| \right) \\
 & + \frac{1}{NP_{IIAC}} \sum_i^{NP_{IIAC}} \left(\left| \frac{IIAC^{exp} - IIAC^{calc}}{IIAC^{exp}} \right| \right)
 \end{aligned} \quad (24)$$

where NP represents the number of experimental points per property.

The objective function assigns different weights depending on the property. It is formulated so that the MIAC and density have twice the weight in the regression process compared to IIAC. The latter were mostly used as indicative to the trend of the different ions. To ensure that this trend will be correct we propose following two different steps in the regression process. First, use only the IIAC and density to evaluate the ionic parameters. This ensures that the IIAC will have the correct trend. Afterwards, using the parameters of the first step as initial estimates, the process is repeated by also utilizing the MIAC. This was the only method where it was possible to get a consistently good representation of all the properties included in the regression. The parameters determined from

regression are tabulated in Table 7. In this table, two approaches with a constant relative permittivity are shown: the parameters of Selam et al. [27] as well as a new set determined in this work. The reasoning behind the calculation of the second set of parameters was fair comparison between the different approaches, as the IIAC had not been included in the regression of the parameters in the work of Selam et al. [27] and their prediction produced the wrong trend, as shown in Fig. 7. In this table, both approaches for the Born diameters are shown, abbreviated HS: the Born diameter is taken equal to the Hard Sphere diameter and RH: the Born diameter is taken from the work of Rashin and Honig [53]. For the models utilizing a constant relative permittivity, the Born term has no contribution to the MIAC, therefore no Born diameters are specified in Table 7. Regarding the trend of the parameters, consistent trends are observed; within the same group, ϵ_{ion} increases from smaller to bigger ions (Li⁺ to K⁺ and Cl⁻ to I⁻), the ion – water interactions, $\epsilon_{ion,water}$, are larger for cations compared to anions and their values also increase in the same group from smaller to bigger ions (Li⁺ to K⁺ and Cl⁻ to I⁻). The segment diameters, σ_{ion} , of cations and anions follow the trend of Pauling radii, apart from Li⁺ that is found to have a bigger ionic diameter compared to Na⁺, without an apparent reason. This was not observed in the previous eSAFT-VR Mie version by Selam et al. [27].

Results for MIAC and IIAC are plotted in Fig. 7 and deviations are tabulated in Table 8 (see also the Supplementary material). All the relative permittivity relations produce good results for both the MIAC, IIAC and densities. The correct trends for the IIAC are followed by all of the approaches, apart from the model of Selam et al. [27], however, when the relative permittivity is constant, the IIAC of potassium salts are less accurate compared to the other approaches, and the model has difficulties achieving the correct trend of the IIAC, as shown in Fig. 7. This is not observed for any other relative permittivity models. The best accuracy is achieved by the MFMR models, especially when the Born diameters of Rashin and Honig [53] are used.

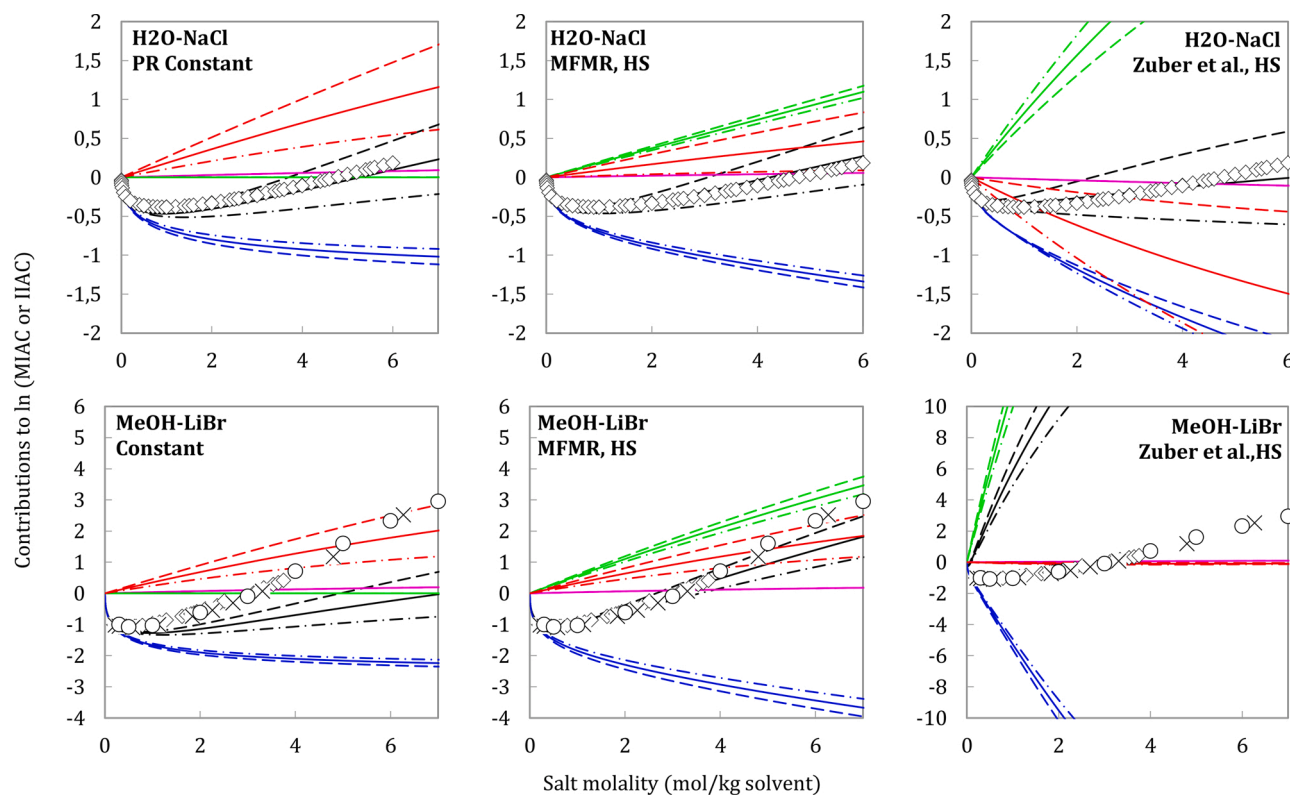


Fig. 9. Contribution of the different terms comprising eSAFT-VR Mie in MIAC (mole fraction scale) using different approaches for the relative permittivity. Points are experimental data, lines are model predictions: solid lines correspond to MIAC, dashed lines to cation IIAC and dashed-dot lines to anion IIAC. Black lines to the total AC, red to the SAFT-VR Mie contribution, blue to the DH contribution, green to the Born contribution and pink to $\ln(Z)$.

3.4. eSAFT-VR Mie modeling of non-aqueous systems

To investigate the effect of the relative permittivity relations in non-aqueous solutions, we have used the models described in Table 7 to predict the MIAC of salts in single solvent solutions of methanol and ethanol. The database of MIAC shown in Table 5 has been used for the non-aqueous systems and the deviations are shown in Table 9 and plotted in Fig. 8 (also see Supplementary Material). To model the non-aqueous solutions the binary interaction parameters between ions and solvent have been set equal to those between ions and water, apart from the model of Selam et al. [27], where specific solvent-ion parameters ($\epsilon_{ion,solvent}/k_B$, shown in Table 10) have been determined by fitting to the available experimental MIAC data. The eSAFT-VR Mie by Selam et al. [27] cannot even correlate MIAC in non-aqueous mixtures, which are severely underpredicted, as shown in Fig. 8. The new parameterization with the constant relative permittivity also fails to capture MIAC in non-aqueous solvents, as shown in the same figure. It seems that using a constant relative permittivity that is salt-concentration independent is the reason for a severe underprediction of MIAC.

In the work of Zuo and Fürst [38] and Zuo et al. [39], the electrolyte EoS of Fürst and Renon has been extended to non-aqueous and mixed solvents. In their work (see Figs. 4 and 5 in the original work [39]), the authors clearly show the importance of the short-range contribution term, SR2, without which it seems impossible to get accurate non-aqueous NaBr MIAC. In our work, the equivalent term to the SR2 is the Born term. And, as we show, it is not possible to extrapolate to non-aqueous solutions when the Born term has no contribution to the MIAC, or in other words when the relative permittivity is constant. Bülow et al. [10] presented similar results when using a constant relative permittivity in their Fig. 7. Therefore, for non-aqueous solutions, the ion-solvent interactions should be accounted for. If a Born term is used for this purpose, it needs to be paired with a salt-composition dependent relative permittivity. Walker et al. [9] arrived at the same conclusion for

the Born term and relative permittivity but from a completely different point of view.

In the case of the MFMR, the non-aqueous MIAC can be predicted with very good accuracy using parameters fitted on aqueous data. Bülow et al. [10] made similar observations with their ePC-SAFT model using the MFMR and they stated that by incorporating a salt-concentration dependent relative permittivity into the Born and the DH terms within the ePC-SAFT framework, they achieved the transferability of ionic parameters to non-aqueous, low permittivity solutions. In our work, we validated their conclusion; indeed, the MFMR is a relative permittivity relation that ensures transferable parameters for eSAFT-VR Mie as well, as shown in Fig. 8. We also offer some possible reasons for the good performance of the MFMR.

When the experimental relative permittivity is used, modelled by the Zuber et al. relation within the eSAFT-VR Mie predictive framework, the MIAC are significantly overpredicted. Such high values for the MIAC would practically mean zero solubility of salts in non-aqueous solvents, which is not the case. The Q-electrolyte model [41], which uses the same relative permittivity relation, showed good MIAC results, however the ionic diameters are solvent specific and fitted to experimental data, so the accuracy of the model could be a result of over-parameterization.

It seems that, in order to get a good extrapolation from aqueous to non-aqueous solvents, the relative permittivity should be a function of the salt concentration, but using the experimental value does not yield the best results. There are two plausible reasons for this observation: a) the kinetic depolarization should not be included in the EoS and b) the relative permittivity cancels out the ion pairing effects. As stated in the introduction, the experimentally measured relative permittivity also contains the kinetic depolarization, which is not a thermodynamic property. In Fig. 2, the kinetic depolarization as determined by Maribo-Mogensen et al. [91] is shown and a MFMR is a good approximation of the dielectric relaxation, or the “thermodynamic part” of the relative permittivity, at least for NaCl in water. It has been previously proposed

that only the thermodynamic part of the relative permittivity should in principle be used for modeling thermodynamic properties within an EoS framework [11]. Another reason for our observation could be the inability of our model to account for ion-pairing in low permittivity media. It is possible, that the good results with the MFMR are a convenient cancelation of errors between an incorrect relative permittivity (meaning not the experimental one) and the formation of ion pairs. The charges of ions that are paired are partially screened by their counter-ion pairs, instead of solvent molecules. This allows additional solvent molecules to rotate according to an external field, increasing the mixture relative permittivity, as compared to a solution of non-paired ions. Since our model belongs to the primitive approach for the relative permittivity, it might be possible to take into account the ion-pairing effect by changing the relative permittivity accordingly.

The different terms contributing to the MIAC calculation with eSAFT-VR Mie are the SAFT-VR Mie [27] terms (association, hard sphere, monomer or dispersion, and chain), the DH and the Born term. The contributions of the different terms with the different approaches for the relative permittivity are shown in Fig. 9. As expected, when the Born term is used with a salt-composition-independent relative permittivity its contribution is zero, and in this case, the SAFT-VR Mie physical contributions counter-balance the DH term. The contribution of the electrolyte terms increases as the dependence of the mixture relative permittivity on the salt concentration increases. Especially for the Zuber et al. relation, the differences between the contribution of the electrolyte term between aqueous and non-aqueous solutions is approximately an order of magnitude. A similar plot, both qualitative and quantitative, was presented by Bulow et al. [10]. Another interesting observation is that neither the Born nor the DH terms deviate significantly between anions and cations. The IIAC trends showing ion preference to the solvent are taken into account due to the (fitted) dispersion term of the model.

4. Conclusions

In this work, eSAFT-VR Mie was extended to low relative permittivity, non-aqueous solutions. The effect of using different relative permittivity relations for the electrolyte solutions was studied, ranging from experimentally measured values to a salt-composition independent relative permittivity. Furthermore, the effect of using different approaches for the ionic diameters in the DH and Born term was evaluated. eSAFT-VR Mie was reparametrized using aqueous Mean Ionic Activity Coefficient (MIAC) and densities with different relations for the relative permittivity. All relations for the relative permittivity yield a relatively accurate representation of the aqueous solutions, with the most accurate one being the mole fraction based mixing rule. Afterwards, the performance of these models on non-aqueous solutions was assessed based on MIAC for methanol and ethanol single-solvent solutions. A mole fraction based mixing rule for the relative permittivity yields the best extrapolation from aqueous to non-aqueous solutions, and achieves quantitative predictions for MIAC of monovalent salts in methanol and ethanol without additional adjustable parameters. On the other hand, the Zuber et al. relation for the relative permittivity significantly overpredicted the MIAC, while the constant relative permittivity underpredicted it. It is concluded that a salt-composition-dependent mixture relative permittivity should be used in EoS to achieve accurate predictions for non-aqueous solutions. However, using the experimental value of the relative permittivity (in the form of the Zuber et al. correlation) does not guarantee better results compared to a mild salt-concentration dependence of the mixture relative permittivity, resembling the thermodynamic contribution, such as the mole fraction mixing rule. Two reasons might be behind this: a) the thermodynamic part of the relative permittivity should be used within the framework of EoS or b) the unaccounted ion-pairing in the solution is cancelled out by a reduced relative permittivity value. Both are reasonable explanations provided in this work, but further research on the relative permittivity and ion-

pairing implementation could shed more light on the subject.

CRediT authorship contribution statement

Nefeli Novak: Methodology, Software, Validation, Formal analysis, Investigation, Writing – original draft, Visualization, Data curation. **Georgios M. Kontogeorgis:** Writing – review & editing, Supervision, Project administration, Funding acquisition. **Marcelo Castier:** Writing – review & editing, Supervision, Project administration. **Ioannis G. Economou:** Resources, Writing – review & editing, Supervision, Project administration.

Declaration of Competing Interest

The authors declare that they have no known competing financial interests or personal relationships that could have appeared to influence the work reported in this paper.

Data Availability

No data was used for the research described in the article.

Acknowledgment

The authors wish to thank the European Research Council (ERC) for funding this research under the European Union's Horizon 2020 research and innovation program (grant agreement no 832460), ERC Advanced Grant project "New Paradigm in Electrolyte Thermodynamics". Open Access funding provided by the Qatar National Library.

Supplementary materials

Supplementary material associated with this article can be found, in the online version, at doi:10.1016/j.fluid.2022.113618.

References

- [1] H. Jiang, A.Z. Panagiotopoulos, I.G. Economou, Modeling of CO₂ solubility in single and mixed electrolyte solutions using statistical associating fluid theory, *Geochim. Cosmochim. Acta* 176 (2016) 185–197, <https://doi.org/10.1016/j.gca.2015.12.023>.
- [2] T. Wendling, E. Risto, T. Krause, L.J. Gooßen, Salt-free strategy for the insertion of CO₂ into C–H bonds: catalytic hydroxymethylation of alkynes, *Chem. – A Eur. J.* 24 (2018) 6019–6024, <https://doi.org/10.1002/chem.201800526>.
- [3] K.S. Pedersen, P.L. Christensen, *Phase Behavior of Petroleum Reservoir Fluids*, CRC Press, Boca Raton, 2006.
- [4] J.M. Míguez, M.C. Dos Ramos, M.M. Piñeiro, F.J. Blas, An examination of the ternary methane + carbon dioxide + water phase diagram using the SAFT-VR approach, *J. Phys. Chem. B* 115 (2011) 9604–9617.
- [5] C.L. Cipolla, E.P. Lolon, J.C. Erdle, B. Rubin, Reservoir modeling in shale-gas reservoirs, *SPE Reserv. Eval. Eng.* 13 (2010) 638–653, <https://doi.org/10.2118/125530-PA>.
- [6] X. Wu, Y. Gong, S. Xu, Z. Yan, X. Zhang, S. Yang, Electrical conductivity of lithium chloride, lithium bromide, and lithium iodide electrolytes in methanol, water, and their binary mixtures, *J. Chem. Eng. Data* 64 (2019) 4319–4329, <https://doi.org/10.1021/acs.jced.9b00405>.
- [7] J.P.G. Villaluenga, B. Seoane, V.M. Barragán, C. Ruiz-Bauzá, Permeation of electrolyte water-methanol solutions through a Nafion membrane, *J. Colloid Interface Sci.* 268 (2003) 476–481, [https://doi.org/10.1016/S0021-9797\(03\)00585-X](https://doi.org/10.1016/S0021-9797(03)00585-X).
- [8] N. Xin, Y. Sun, C.J. Radke, J.M. Prausnitz, Osmotic and activity coefficients for five lithium salts in three non-aqueous solvents, *J. Chem. Thermodyn.* 132 (2019) 83–92, <https://doi.org/10.1016/j.jct.2018.12.016>.
- [9] P.J. Walker, X. Liang, G.M. Kontogeorgis, Importance of the relative static permittivity in electrolyte SAFT-VR Mie equations of state, *Fluid Phase Equilib* 551 (2022), 113256, <https://doi.org/10.1016/j.fluid.2021.113256>.
- [10] M. Bülow, M. Ascani, C. Held, ePC-SAFT advanced - Part I: Physical meaning of including a concentration-dependent dielectric constant in the Born term and in the Debye-Hückel theory, *Fluid Phase Equilib* 535 (2021), 112967, <https://doi.org/10.1016/j.fluid.2021.112967>.
- [11] G.M. Kontogeorgis, B. Maribo-Mogensen, K. Thomsen, The Debye-Hückel theory and its importance in modeling electrolyte solutions, *Fluid Phase Equilib* 462 (2018) 130–152, <https://doi.org/10.1016/j.fluid.2018.01.004>.

- [12] C.A. Haynes, J. Newman, On converting from the McMillan-Mayer framework: I. Single-solvent system, *Fluid Phase Equilib* 145 (1998) 255–268, [https://doi.org/10.1016/S0378-3812\(97\)00335-x](https://doi.org/10.1016/S0378-3812(97)00335-x).
- [13] M.P. Breil, J.M. Møllerup, The McMillan-Mayer framework and the theory of electrolyte solutions, *Fluid Phase Equilib* 242 (2006) 129–135, <https://doi.org/10.1016/j.fluid.2006.01.018>.
- [14] M. Michelsen, J. Møllerup, *Thermodynamic Modelling: Fundamentals and Computational Aspects*, 2nd ed., Tie-Line Publications, Denmark, 2007.
- [15] S. Ahmed, N. Ferrando, J.C. de Hemptinne, J.P. Simonin, O. Bernard, O. Baudouin, Modeling of mixed-solvent electrolyte systems, *Fluid Phase Equilib* 459 (2018) 138–157, <https://doi.org/10.1016/j.fluid.2017.12.002>.
- [16] B. Maribo-Mogensen, G.M. Kontogeorgis, K. Thomsen, Modeling of dielectric properties of complex fluids with an equation of state, *J. Phys. Chem. B* 117 (2013) 3389–3397, <https://doi.org/10.1021/jp310572q>.
- [17] P. Debye, E. Hückel, The theory of electrolytes: I. lowering of freezing point and related phenomena, *Phys. Z.* 24 (1923) 185–206.
- [18] M. Born, Volumen und Hydratationswärme der Ionen, *Zeitschrift Für Phys.* 1 (1920) 45–48, <https://doi.org/10.1007/BF01881023>.
- [19] L. Sun, X. Liang, N. von Solms, G.M. Kontogeorgis, Analysis of some electrolyte models including their ability to predict the activity coefficients of individual ions, *Ind. Eng. Chem. Res.* 59 (2020) 11790–11809, <https://doi.org/10.1021/acs.iecr.0c00980>.
- [20] M.D. Olsen, G.M. Kontogeorgis, X. Liang, N. Von Solms, Investigation of the performance of e-CPA for a wide range of properties for aqueous NaCl solutions, *Fluid Phase Equilib* (2021), 113167, <https://doi.org/10.1016/j.fluid.2021.113167>.
- [21] P. Wang, A. Anderko, Computation of dielectric constants of solvent mixtures and electrolyte solutions, *Fluid Phase Equilib* 186 (2001) 103–122, [https://doi.org/10.1016/S0378-3812\(01\)00507-6](https://doi.org/10.1016/S0378-3812(01)00507-6).
- [22] B. Maribo-Mogensen, G.M. Kontogeorgis, K. Thomsen, Comparison of the Debye-Hückel and the mean spherical approximation theories for electrolyte solutions, *Ind. Eng. Chem. Res.* 51 (2012) 5353–5363, <https://doi.org/10.1021/ie2029943>.
- [23] S. Herzog, J. Gross, W. Arit, Equation of state for aqueous electrolyte systems based on the semirestricted non-primitive mean spherical approximation, *Fluid Phase Equilib* 297 (2010) 23–33, <https://doi.org/10.1016/j.fluid.2010.05.024>.
- [24] Z. Liu, W. Wang, Y. Li, An equation of state for electrolyte solutions by a combination of low-density expansion of non-primitive mean spherical approximation and statistical associating fluid theory, *Fluid Phase Equilib* 227 (2005) 147–156, <https://doi.org/10.1016/j.fluid.2004.11.007>.
- [25] G. Das, M.C. dos Ramos, C. McCabe, Predicting the thermodynamic properties of experimental mixed-solvent electrolyte systems using the SAFT-VR+DE equation of state, *Fluid Phase Equilib* 460 (2018) 105–118, <https://doi.org/10.1016/j.fluid.2017.11.017>.
- [26] G. Das, S. Hlushak, C. McCabe, A SAFT-VR+DE equation of state based approach for the study of mixed dipolar solvent electrolytes, *Fluid Phase Equilib* 416 (2016) 72–82, <https://doi.org/10.1016/j.fluid.2015.11.027>.
- [27] M.A. Selam, I.G. Economou, M. Castier, A thermodynamic model for strong aqueous electrolytes based on the eSAFT-VR Mie equation of state, *Fluid Phase Equilib* 464 (2018) 47–63, <https://doi.org/10.1016/j.fluid.2018.02.018>.
- [28] N. Novak, G.M. Kontogeorgis, M. Castier, I.G. Economou, Modeling of Gas Solubility in Aqueous Electrolyte Solutions with the eSAFT-VR Mie Equation of State, *Ind. Eng. Chem. Res.* 60 (2021) 15327–15342, <https://doi.org/10.1021/acs.iecr.1c02923>.
- [29] C. Held, L.F. Cameretti, G. Sadowski, Modeling aqueous electrolyte solutions. Part 1. Fully dissociated electrolytes, *Fluid Phase Equilib* 270 (2008) 87–96, <https://doi.org/10.1016/j.fluid.2008.06.010>.
- [30] J.M.A. Schreckenber, S. Dufal, A.J. Haslam, C.S. Adjiman, G. Jackson, A. Galindo, Modelling of the thermodynamic and solvation properties of electrolyte solutions with the statistical associating fluid theory for potentials of variable range, *Mol. Phys.* 112 (2014) 2339–2364, <https://doi.org/10.1080/00268976.2014.910316>.
- [31] D.K. Eriksen, G. Lazarou, A. Galindo, G. Jackson, C.S. Adjiman, A.J. Haslam, Development of intermolecular potential models for electrolyte solutions using an electrolyte SAFT-VR Mie equation of state, *Mol. Phys.* 114 (2016) 2724–2749, <https://doi.org/10.1080/00268976.2016.1236221>.
- [32] A. Zuber, L. Cardozo-Filho, V.F. Cabral, R.F. Checoni, M. Castier, An empirical equation for the dielectric constant in aqueous and nonaqueous electrolyte mixtures, *Fluid Phase Equilib* 376 (2014) 116–123, <https://doi.org/10.1016/j.fluid.2014.05.037>.
- [33] R. Inchehel, J.C. de Hemptinne, W. Fürst, The simultaneous representation of dielectric constant, volume and activity coefficients using an electrolyte equation of state, *Fluid Phase Equilib* 271 (2008) 19–27, <https://doi.org/10.1016/j.fluid.2008.06.013>.
- [34] J. Rozmus, J.C. de Hemptinne, A. Galindo, S. Dufal, P. Mougin, Modeling of strong electrolytes with ePPC-SAFT up to high temperatures, *Ind. Eng. Chem. Res.* 52 (2013) 9979–9994, <https://doi.org/10.1021/ie303527j>.
- [35] B. Maribo-Mogensen, Development of an Electrolyte CPA Equation of state for Applications in the Petroleum and Chemical Industries, DTU Chemical Engineering, Department of Chemical and Biochemical Engineering, 2014. PhD thesis.
- [36] J.S. Roa Pinto, N. Ferrando, J.-C. de Hemptinne, A. Galindo, Temperature dependence and short-range electrolytic interactions within the e-PPC-SAFT framework, *Fluid Phase Equilib* 560 (2022), 113486, <https://doi.org/10.1016/j.fluid.2022.113486>.
- [37] C. Held, Thermodynamic gModels and equations of state for electrolytes in a water-poor medium: a review, *J. Chem. Eng. Data* 65 (2020) 5073–5082, <https://doi.org/10.1021/acs.jced.0c00812>.
- [38] Y.X. Zuo, W. Fürst, Prediction of vapor pressure for nonaqueous electrolyte solutions using an electrolyte equation of state, *Fluid Phase Equilib.* 138 (1997) 87–104, [https://doi.org/10.1016/S0378-3812\(97\)00145-3](https://doi.org/10.1016/S0378-3812(97)00145-3).
- [39] J.Y. Zuo, D. Zhang, W. Fürst, Extension of the electrolyte EOS of furst and renon to mixed solvent electrolyte systems, *Fluid Phase Equilib.* 175 (2000) 285–310, [https://doi.org/10.1016/S0378-3812\(00\)00463-5](https://doi.org/10.1016/S0378-3812(00)00463-5).
- [40] M. Ascani, C. Held, Prediction of salting-out in liquid-liquid two-phase systems with ePC-SAFT: Effect of the Born term and of a concentration-dependent dielectric constant, *Zeitschrift Fur Anorg. Und Allg. Chemie* 647 (2021) 1305–1314, <https://doi.org/10.1002/zaac.202100032>.
- [41] A. Zuber, R.F. Checoni, M. Castier, Thermodynamic properties of nonaqueous single salt solutions using the Q-electrolattice equation of state, *Brazilian J. Chem. Eng.* 32 (2015) 637–646, <https://doi.org/10.1590/0104-6632.20150323s00003389>.
- [42] C. Held, A. Prinz, V. Wallmeyer, G. Sadowski, Measuring and modeling alcohol/salt systems, *Chem. Eng. Sci.* 68 (2012) 328–339, <https://doi.org/10.1016/j.ces.2011.09.040>.
- [43] N. Papaiconomou, J.P. Simonin, O. Bernard, W. Kunz, MSA-NRTL model for the description of the thermodynamic properties of electrolyte solutions, *Phys. Chem. Chem. Phys.* 4 (2002) 4435–4443, <https://doi.org/10.1039/b204841h>.
- [44] S. Müller, A. González de Castilla, C. Taeschler, A. Klein, I. Smirnova, Calculation of thermodynamic equilibria with the predictive electrolyte model COSMO-RS-ES: Improvements for low permittivity systems, *Fluid Phase Equilib* 506 (2020) 1–11, <https://doi.org/10.1016/j.fluid.2019.112368>.
- [45] M. Bülow, M. Ascani, C. Held, Fluid phase equilibria ePC-SAFT advanced – Part II: application to salt solubility in ionic and organic solvents and the impact of ion pairing, *Fluid Phase Equilib* 537 (2021), 112989, <https://doi.org/10.1016/j.fluid.2021.112989>.
- [46] I.K. Nikolaidis, N. Novak, G.M. Kontogeorgis, I.G. Economou, Rigorous Phase Equilibrium Calculation Methods for Strong Electrolyte Solutions: The Isothermal Flash, *Fluid Phase Equilib* 558 (2022), 113441, <https://doi.org/10.1016/j.fluid.2022.113441>.
- [47] T. Lafitte, A. Apostolou, C. Avendaño, A. Galindo, C.S. Adjiman, E.A. Müller, G. Jackson, Accurate statistical associating fluid theory for chain molecules formed from Mie segments, *J. Chem. Phys.* 139 (2013), 154504, <https://doi.org/10.1063/1.4819786>.
- [48] S. Dufal, T. Lafitte, A.J. Haslam, A. Galindo, G.N.I. Clark, C. Vega, G. Jackson, The A in SAFT: developing the contribution of association to the Helmholtz free energy within a Wertheim TPT1 treatment of generic Mie fluids, *Mol. Phys.* 113 (2015) 948–984, <https://doi.org/10.1080/00268976.2015.1029027>.
- [49] S. Dufal, T. Lafitte, A. Galindo, G. Jackson, A.J. Haslam, Developing intermolecular-potential models for use with the SAFT-VR Mie equation of state, *AIChE J* 61 (2015) 2891–2912.
- [50] G.H. Hudson, J.C. McCoubrey, Intermolecular forces between unlike molecules. A more complete form of the combining rules, *Trans. Faraday Soc.* 56 (1960) 761–766, <https://doi.org/10.1039/TF9605600761>.
- [51] A.J. Haslam, A. Galindo, G. Jackson, Prediction of binary intermolecular potential parameters for use in modelling fluid mixtures, *Fluid Phase Equilib* 266 (2008) 105–128, <https://doi.org/10.1016/j.fluid.2008.02.004>.
- [52] G.M. Kontogeorgis, G.K. Folas, Thermodynamic Models for Industrial Applications: From Classical and Advanced Mixing Rules to Association Theories, John Wiley & Sons, 2009, <https://doi.org/10.1002/9780470747537>.
- [53] A. Rashin, B. Honig, Reevaluation of the Born model of ion hydration, *J. Phys. Chem.* 89 (1985) 5588–5593, <https://doi.org/10.1021/j100272a006>.
- [54] K. Thomsen, *Electrolyte Solutions: Thermodynamics, Crystallization, Separation methods*, Technical University of Denmark, 2009.
- [55] B. Long, D. Zhao, W. Liu, Thermodynamics studies on the solubility of inorganic salt in organic solvents: Application to KI in organic solvents and water-ethanol mixtures, *Ind. Eng. Chem. Res.* 51 (2012) 9456–9467, <https://doi.org/10.1021/ie301000b>.
- [56] J. Barthel, G. Laueremann, Vapor pressure measurements on non-aqueous electrolyte solutions. Part 3: Solutions of sodium iodide in ethanol, 2-propanol, and acetonitrile, *J. Solution Chem.* 15 (1986) 869–877, <https://doi.org/10.1007/bf00646093>.
- [57] F.J. Passamonti, M.R.G. de Chialvo, A.C. Chialvo, Thermodynamically consistent equations for the accurate description of the logarithm of the solvent activity and related properties of electrolyte solutions with a unique set of parameters: critical analysis of the mean activity coefficient evaluation, *J. Solution Chem.* 49 (2020) 695–714.
- [58] J. Barthel, R. Neueder, G. Laueremann, Vapor pressures of non-aqueous electrolyte solutions. Part 1. Alkali metal salts in methanol, *J. Solution Chem.* 14 (1985) 621–633, <https://doi.org/10.1007/BF00646055>.
- [59] J. Barthel, G. Laueremann, R. Neueder, Vapor pressure measurements on non-aqueous electrolyte solutions. Part 2. Tetraalkylammonium salts in methanol. Activity coefficients of various 1-1 electrolytes at high concentrations, *J. Solution Chem.* 15 (1986) 851–867, <https://doi.org/10.1007/BF00646092>.
- [60] J. Barthel, R. Neueder, H. Poepeke, H. Wittmann, Osmotic coefficients and activity coefficients of nonaqueous electrolyte solutions. Part 4. Lithium bromide, tetrabutylammonium bromide, and tetrabutylammonium perchlorate in acetone, *J. Solution Chem.* 28 (1999) 1277–1287, <https://doi.org/10.1023/A:1021791823158>.
- [61] J. Barthel, R. Neueder, H. Wittmann, Osmotic coefficients and activity coefficients of nonaqueous electrolyte solutions. Part 3. Tetraalkylammonium bromides in ethanol and 2-propanol, *J. Solution Chem.* 28 (1999) 1263–1276, <https://doi.org/10.1023/A:1021741006320>.

- [62] J. Barthel, R. Neueder, H. Poepke, H. Wittmann, Osmotic and activity coefficients of nonaqueous electrolyte solutions. 1. Lithium perchlorate in the protic solvents methanol, ethanol, and 2-propanol, *J. Solution Chem.* 27 (1998) 1055–1066, <https://doi.org/10.1023/A:1022637316064>.
- [63] K. Nasirzadeh, N. Papaiconomou, R. Neueder, W. Kunz, Vapor pressures, osmotic and activity coefficients of electrolytes in protic solvents at different temperatures, 1. Lithium Bromide in Methanol, *J. of Solution Chem.* 33 (2004) 227–245, <https://doi.org/10.1023/B:JOSL.0000035357.18045.0d>.
- [64] K. Nasirzadeh, R. Neueder, W. Kunz, Vapor pressures, osmotic and activity coefficients of electrolytes in protic solvents at different temperatures. 2. Lithium bromide in ethanol, *J. Solution Chem.* 33 (2004) 1429–1446, <https://doi.org/10.1007/s10953-004-1057-9>.
- [65] K. Nasirzadeh, R. Neueder, W. Kunz, Vapor pressures, osmotic and activity coefficients of electrolytes in protic solvents at different temperatures. 3. Lithium Bromide in 2-Propanol, 34 (2005) 9–24, <https://doi.org/10.1007/s10953-005-2024-9>.
- [66] K. Nasirzadeh, R. Neueder, W. Kunz, Vapor pressures, osmotic and activity coefficients for (LiBr+ acetonitrile) between the temperatures (298.15 and 343.15) K, *J. Chem. Thermodyn.* 36 (2004) 511–517.
- [67] J.T. Safarov, Vapor pressures of lithium bromide or lithium chloride and ethanol solutions, *Fluid Phase Equilib.* 243 (2006) 38–44, <https://doi.org/10.1016/j.fluid.2006.02.012>.
- [68] J.T. Safarov, Vapor pressure measurements of binary solutions of CaCl₂ with methanol and ethanol at T = (298.15 to 323.15) K using a static method, *J. Chem. Eng. Data.* 51 (2006) 360–365, <https://doi.org/10.1021/je0502086>.
- [69] J.T. Safarov, Study of thermodynamic properties of binary solutions of lithium bromide or lithium chloride with methanol, *Fluid Phase Equilib.* 236 (2005) 87–95, <https://doi.org/10.1016/j.fluid.2005.07.002>.
- [70] M.T. Zafarani-Moattar, M. Aria, Isopiestic determination of osmotic and activity coefficients for solutions of LiCl, LiBr, and LiNO₃ in 2-propanol at 25°C, *J. Solution Chem.* 30 (2001) 351–363, <https://doi.org/10.1023/A:1010327206913>.
- [71] P.A. Skabichevskii, Osmotic coefficients of lithium chloride and bromide solutions in methanol, *Russ. J. Phys. Chem.* 43 (1969) 1432.
- [72] F. Hernández-Luis, M.V. Vázquez, M.A. Esteso, Activity coefficients for NaF in methanol-water and ethanol-water mixtures at 25°C, *J. Mol. Liq.* 108 (2003) 283–301, [https://doi.org/10.1016/S0167-7322\(03\)00187-9](https://doi.org/10.1016/S0167-7322(03)00187-9).
- [73] W. Yan, Y. Xu, S. Han, Activity Coefficients of Sodium Chloride in Methanol-Water Mixed Solvents at 298.15 K, *Chinese Sci. Abstr. Ser. B* (1995) 17.
- [74] M.A. Esteso, O.M. Gonzalez-Diaz, F.F. Hernandez-Luis, L. Fernandez-Merida, Activity coefficients for NaCl in ethanol-water mixtures at 25°C, *J. Solution Chem.* 18 (1989) 277–288.
- [75] S. Han, H. Pan, Thermodynamics of the sodium bromide-methanol-water and sodium bromide-ethanol-water two ternary systems by the measurements of electromotive force at 298.15 K, *Fluid Phase Equilib.* 83 (1993) 261–270.
- [76] O.M. Gonzalez-Diaz, L. Fernández-Mérida, F. Hernández-Luis, M.A. Esteso, Activity coefficients for NaBr in ethanol-water mixtures at 25°C, *J. Solution Chem.* 24 (1995) 551–563, <https://doi.org/10.1007/BF00973206>.
- [77] L. Malahias, O. Popovych, Activity coefficients and transfer free energies of potassium chloride in methanol-water solvents at 25°C, *J. Chem. Eng. Data.* 27 (1982) 105–109, <https://doi.org/10.1021/je00028a001>.
- [78] Y.G. Vlasov, P.P. Antonov, Activity of Methanol and activity coefficients of salts in NaCl-Methanol and NaBr-Methanol solutions at 25 degrees C, *Zhurnal Fiz. Khimii.* 47 (1973) 2264–2266.
- [79] R.R. Kolhapurkar, P.K. Patil, D.H. Dagade, K.J. Patil, Studies of thermodynamic properties of binary and ternary methanolic solutions containing KBr and 18-Crown-6 at 298.15 K, *J. Solution Chem.* 35 (2006) 1357–1376, <https://doi.org/10.1007/s10953-006-9066-5>.
- [80] B. Long, Experimental studies and thermodynamic modeling of the solubilities of potassium nitrate, potassium chloride, potassium bromide, and sodium chloride in dimethyl sulfoxide, *Ind. Eng. Chem. Res.* 50 (2011) 7019–7026, <https://doi.org/10.1021/ie102134g>.
- [81] M. Li, L. Wang, K. Wang, B. Jiang, J. Gmehling, Experimental measurement and modeling of solubility of LiBr and LiNO₃ in methanol, ethanol, 1-propanol, 2-propanol and 1-butanol, *Fluid Phase Equilib.* 307 (2011) 104–109, <https://doi.org/10.1016/j.fluid.2011.03.017>.
- [82] S.H. Saravi, A.Z. Panagiotopoulos, Activity Coefficients and Solubilities of NaCl in Water–Methanol Solutions from Molecular Dynamics Simulations, *J. Phys. Chem. B.* (2022), <https://doi.org/10.1021/acs.jpcc.2c00813>.
- [83] K. Thomsen, Available at, CERE Electrolyte Database, 2014, <http://www.cere.dtu.dk/Expertise/Dat>.
- [84] M.T. Zafarani-Moattar, K. Nasirzade, Osmotic coefficient of methanol + LiCl, + LiBr, and + LiCH₃COO at 25°C, *J. Chem. Eng. Data.* 43 (1998) 215–219, <https://doi.org/10.1021/je970193e>.
- [85] J. Gmehling, Dortmund Data Bank, 2022.
- [86] M. Li, L. Wang, K. Wang, B. Jiang, Experimental measurement and modeling of solubility of LiBr and LiNO₃ in methanol, ethanol, 1-propanol, 2-propanol and 1-butanol, *Fluid Phase Equilib.* 307 (2011) 104–109, <https://doi.org/10.1016/j.fluid.2011.03.017>.
- [87] M. Bülow, X. Ji, C. Held, Incorporating a concentration-dependent dielectric constant into ePC-SAFT. An application to binary mixtures containing ionic liquids, *Fluid Phase Equilib.* 492 (2019) 26–33.
- [88] C. Andeen, J. Fontanella, D. Schuele, Low-frequency dielectric constant of LiF, NaF, NaCl, NaBr, KCl, and KBr by the method of substitution, *Phys. Rev. B.* 2 (1970) 5068–5073, <https://doi.org/10.1103/PhysRevB.2.5068>.
- [89] J. Vincze, M. Valiskó, D. Boda, The nonmonotonic concentration dependence of the mean activity coefficient of electrolytes is a result of a balance between solvation and ion-ion correlations, *J. Chem. Phys.* 133 (2010), <https://doi.org/10.1063/1.3489418>.
- [90] I.Y. Shilov, A.K. Lyashchenko, The role of concentration dependent static permittivity of electrolyte solutions in the Debye-Hückel Theory, *J. Phys. Chem. B.* 119 (2015) 10087–10095.
- [91] B. Maribo-Mogensen, G.M. Kontogeorgis, K. Thomsen, Modeling of dielectric properties of aqueous salt solutions with an equation of state, *J. Phys. Chem. B.* 117 (2013) 10523–10533, <https://doi.org/10.1021/jp403375t>.
- [92] J.-P.P. Simonin, O. Bernard, L. Blum, Ionic solutions in the binding mean spherical approximation: thermodynamic properties of mixtures of associating electrolytes, *J. Phys. Chem. B.* 103 (1999) 699–704, <https://doi.org/10.1021/jp9833000>.
- [93] B. Maribo-Mogensen, K. Thomsen, G.M. Kontogeorgis, An electrolyte CPA equation of state for mixed solvent electrolytes, *AIChE J.* 61 (2015) 2933–2950, <https://doi.org/10.1002/aic.14829>.
- [94] X. Courtial, N. Ferrando, J.C. de Hemptinne, P. Mougin, Electrolyte CPA equation of state for very high temperature and pressure reservoir and basin applications, *Geochim. Cosmochim. Acta.* 142 (2014) 1–14, <https://doi.org/10.1016/j.gca.2014.07.028>.
- [95] C. Held, T. Reschke, S. Mohammad, A. Luza, G. Sadowski, EPC-SAFT revised, *Chem. Eng. Res. Des.* 92 (2014) 2884–2897, <https://doi.org/10.1016/j.cherd.2014.05.017>.
- [96] G. Wilczek-Vera, E. Rodil, J.H. Vera, On the activity of ions and the junction potential: revised values for all data, *AIChE J.* 50 (2004) 445–462, <https://doi.org/10.1002/aic.10039>.